



A Review of Energy Storage Mechanisms in Aqueous Aluminium Technology

N. Melzack* and R. G. A. Wills

Energy Technology Research Group, Mechanical Engineering, University of Southampton, Southampton, United Kingdom

This systematic review covers the developments in aqueous aluminium energy storage technology from 2012, including primary and secondary battery applications and supercapacitors. Aluminium is an abundant material with a high theoretical volumetric energy density of -8.04 Ah cm^{-3} . Combined with aqueous electrolytes, which have twice the ionic storage potential as non-aqueous versions, this technology has the potential to serve many energy storage needs. The charge transfer mechanisms are discussed in detail with respect to aqueous aluminium-ion secondary batteries, where most research has focused in recent years. TiO_2 nanopowders have shown to be promising negative electrodes, with the potential for pseudocapacitive energy storage in aluminium-ion cells. This review summarises the advances in Al-ion systems using aqueous electrolytes, focusing on electrochemical performance.

Keywords: aluminium-ion, energy storage, aluminium-ion batteries, aluminium-air, aqueous aluminium

OPEN ACCESS

Edited by:

Paul Shearing,
University College London,
United Kingdom

Reviewed by:

Franky Esteban Bedoya-Lora,
University of Antioquia, Colombia
Muhammad Sufyan Javed,
Jinan University, China
Jacob Lamb,
Norwegian University of Science and
Technology, Norway

*Correspondence:

N. Melzack
n.melzack@soton.ac.uk

Specialty section:

This article was submitted to
Electrochemical Engineering,
a section of the journal
Frontiers in Chemical Engineering

Received: 16 September 2021

Accepted: 18 March 2022

Published: 27 April 2022

Citation:

Melzack N and Wills RGA (2022) A
Review of Energy Storage
Mechanisms in Aqueous
Aluminium Technology.
Front. Chem. Eng. 4:778265.
doi: 10.3389/fceng.2022.778265

1 INTRODUCTION

Sustainable economies depend on the increasing reliability and use of energy storage (UK Government, 2008; Tang et al., 2013; IPCC et al., 2014; UK Government, 2019; Larcher and Tarascon, 2015). Many energy storage devices are available. However, Li-ion battery technology has accelerated the development of portable devices, electronic vehicles, and grid storage in the last 2 decades (Narins, 2017). Currently, this technology is hard to recycle and relies on sparse and often politicised resources (Prior et al., 2013; Maxwell, 2015; Huang et al., 2018; Ciez and Whitacre, 2019). In order to further our sustainable development, it is important to co-develop our batteries to be easier to recycle and have a lower environmental footprint. In this review, aluminium-based batteries operating with an aqueous electrolyte are evaluated as one such battery technology.

Secondary aluminium-ion (Al-ion) batteries have not reached wide-scale commercial viability yet and are often grouped together with other multivalent metal ion systems in the literature (such as Mg and Ca) (Larcher and Tarascon, 2015; Chao et al., 2020). However, aluminium is the most abundant metal in the Earth's crust (8.1% wt) and the third most abundant element (CHEMnetBASE, 2016). There are already established mining, production, and recycling industries for aluminium (Butterwick and Smith, 1986; USGS, 2020), hinting at an easy and sustainable development roadmap ahead for utilising Al-ion technology within a circular economy.

The electronic configuration of aluminium is $1s^2 2s^2 2p^6 3s^2 3p^1$. The first three ionisation energies for aluminium are 578, 1817, and 2,745 kJ mol^{-1} , while subsequent ionisation energies are a greater order of magnitude. The Al^{3+} ion has the same stable electronic configuration as atomic neon and is the most common valence state for aluminium. This trivalent Al^{3+} ion is, therefore, capable of three electron transfers per ion, unlike lithium's monovalent Li^+ ; that is, one Al-ion is equivalent to three

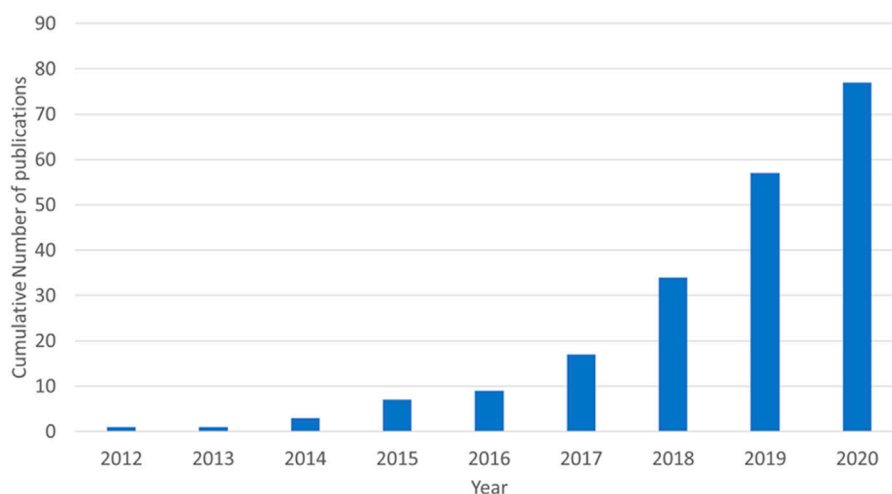


FIGURE 1 | Cumulative number of original research papers published in English from 2012 to 2020 (assessed through Google Scholar search).

Li-ions in terms of charge transfer. While this review is not a direct comparison with Li-ion technology, it is useful to understand where Al-ion sits with regard to the present industry leader.

The ionic radius of Al is slightly smaller than Li, leading to a high charge density, meaning more charge transfer can occur with no increase in a physical restriction to electrodes. Additionally, Al has a high density (2.7 g cm^{-3} at 25°C), which leads to a volumetric energy density of almost four times lithium, 8.04 Ah cm^{-3} and 2.06 Ah cm^{-3} , respectively (Das et al., 2017; Elia et al., 2021; Faegh et al., 2021). Metallic Al also has a high theoretical capacity and density ($2,981 \text{ mA h g}^{-1}$ and $4,140 \text{ Wh kg}^{-1}$, respectively). This, combined with the high abundance, safety, and well-established recyclability, makes the Al-ion a great all-rounder as a charge carrier.

Two challenges arise with the higher charge density for intercalation-type processes: 1) the high charge density means it is difficult for Al^{3+} to lose its coordinating ligands in the solvated state and 2) while intercalating, the Al^{3+} ions can distort the lattice structure of electrodes. The former negates the advantage of the small ionic radius of Al^{3+} , while the latter can reduce the lifetime significantly as the lattice distortions accumulate with each cycle.

This review will cover three types of electrochemical energy storage devices utilising aluminium ions in aqueous electrolytes: rechargeable batteries, non-rechargeable batteries, and capacitors. The capacitor section will include devices named supercapacitors, ultracapacitors, capatteries, and cabatteries. The key component in defining a capacitor, for the purpose of this review, is that the primary form of energy storage is through charge separation. Capatteries are defined as a capacitor that shows faradaic redox reactions in addition to the charge separation. Cabatteries primarily are batteries in which the double layer capacitance has a significant role in the charge storage. In recent years, the number of original research published on aqueous aluminium energy storage has increased significantly. **Figure 1** shows that,

from the single paper published by Liu et al. (2012), there were 77 total publications by the end of 2020.

Batteries are electrochemical storage devices relying primarily on the faradaic redox reaction as a means of charge storage and transfer. Secondary batteries, which facilitate reversible redox reactions, can be charged/discharged multiple times throughout their lifetime. These are rechargeable batteries. Primary batteries are non-reversible and thus can only be discharged a single time in their lifetime (i.e., non-rechargeable).

2 AQUEOUS ELECTROLYTES

An aqueous electrolyte uses water as the solvent for various ionic salts. These electrolytes are often safer than ionic liquids, or non-aqueous electrolytes, due to their low flammability and ease of handling (Chao et al., 2020). Ionic electrolytes, such as those in lithium-ion batteries, can emit volatile, flammable, and toxic solvents when punctured, as well as being hazardous to work with for second-life or recycling applications (Christensen et al., 2021; Larsson et al., 2018). The solvent in aqueous electrolytes, water, is low cost, is widely available, and does not require complex manufacturing or storage (compared to other electrolytes) (Gür, 2018). This already shows advantages in the economic and social (safety) aspects of battery development. However, while cheaper in absolute terms, when considering cost per kW or kWh, it is not yet comparable to non-aqueous commercial batteries. Commercial non-aqueous Li-ion batteries production is expected to cost $\$362/\text{kWh}$, $\$1,446/\text{kWh}$ in 2025 (Mongrid et al., 2019), compared to an aqueous commercial Pb-acid battery, which is expected to cost $\$464/\text{kWh}$, $\$1,845/\text{kWh}$ (United States Department of Energy, 2019).

There are performance reasons for not using aqueous electrolytes. The main reason is the narrow electrochemical stability window (ESW) of water, about 1.23 V. Beyond this point, water electrolysis occurs, and the H_2O decomposes into its constituent parts (Zhang H.

TABLE 1 | Typical ESW for certain electrolytes

Electrolyte	Type	ESW	Reference
Lithium salts	Ionic liquid	4–6 V	Gores et al. (2011)
PAN-gels	Polymer/aqueous	>4.5 V	Gray and Armand (2011); Wang et al. (2019)
Cross-linked	Polymer	3.9 V	Gray and Armand, (2011)
Ionic salt	aqueous	1.23 V	Dell (1996)
WISE	aqueous	3–4 V	Suo et al. (2017); Yang et al. (2017)

et al., 2020). This would limit the energy density of cells constructed in this manner. However, research establishes that a diluted aqueous electrolyte can have an ESW of up to 2 V and even higher with different salt concentrations, promising further development (Suo et al., 2015). A comparison of ESWs for other electrolytes is shown in **Table 1**. Lithium salts in an ionic liquid are used in Li-ion commercial batteries today. They have a high ESW and can, therefore, deliver higher voltages with fewer cells in series. Polymer and gel-type electrolytes are still in their development stage and offer the advantage of a high ESW with lower flammability. However, they are currently not used commercially. From **Table 1**, the aqueous WISE (water in salt electrolyte), in which the salt is saturated, have the potential for higher ESWs, but they are still in the development phase.

Regardless of this low ESW, there is still high demand for aqueous electrolyte development. The potential ionic storage of such electrolytes is two orders of magnitude higher than that of organic non-aqueous electrolytes, which could enable far higher power capability (Zhang H. et al., 2020). There has been an increase in aqueous electrolytes studied for Zn-ion (Wu B et al., 2021; Javed et al., 2020), Na-ion (Jin T. et al., 2021; Tapia-Ruiz et al., 2021), and Li-ion batteries (Cresce and Xu, 2021).

Other limiting factors not bespoke to aqueous electrolytes also apply. Corrosion of electrodes is likely in protic electrolytes, while dendrite formation on electrodes is more likely in alkaline electrolytes (Zhang H. et al., 2020; Chao et al., 2020). These both limit lifetime and discharge voltage obtained over time.

Furthermore, in terms of sustainability, the energy density obtained is not the most key factor. Long-lasting, reliable, safe, cost-effective, and scalable designs are far more critical. Therefore, the narrow ESW, while being widened as new research is published, is by no means a reason to disregard aqueous electrolytes (Posada et al., 2017).

It is near impossible to fully evaluate the aqueous electrolyte in isolation. It forms part of a complex system. With regard to aluminium, few materials have been identified as suitable electrodes that can both operate within the ESW and accommodate the large charge density. Thus, the number of suitable electrodes is being added currently, and this review will discuss some key developments in electrode material and the charge and degradation mechanisms found.

3 MECHANISM IDENTIFICATION IN SECONDARY BATTERIES

The following section discusses aqueous Al-ion secondary batteries, specifically the negative and positive electrode

materials that have been studied, their reported performance, and the charge storage mechanisms involved. The most common electrode materials and electrolytes studied are presented in **Figure 2**, with detailed tables summarising key findings in **Supplementary Table S1** for negative electrode materials and **Supplementary Table S2** for the positive electrode materials.

3.1 Negative Electrode

The negative electrode always has a more negative potential than the positive electrode when in a full cell. Sometimes this is referred to as the anode. However, for secondary cells, because both reduction and oxidation take place at the electrode depending on whether the cell is discharging or charging, it can be confusing to refer to it as the anode. Hence, the negative electrode will be used throughout this section. **Supplementary Table S1** summarises the materials that have, to date, been studied as a negative electrode for an aqueous aluminium-ion cell. It is important to understand the difference between electrodes tested as 'half-cells' and full cells in terms of the capacities and fade values ascertained. For a half-cell, only the electrode testing will influence the capacity and fade characteristics reported. However, with a full cell, both the positive and negative electrodes will have an influence and the reported capacities are for the whole cell, not just the electrode highlighted in the table. For example, Holland et al. (2018a) studied TiO₂ in a full cell with a copper hexacyanoferrate (CuHCF) positive electrode and found a cycle life of 1,750 cycles and a Coulombic efficiency of ~90%. However, in a half-cell with the same conditions, 5,000 cycles were possible with ~99% Coulombic efficiency (Holland et al., 2018b). Most studies to date have focussed on TiO₂ as a negative active material, with MoO₃ being the next most cited material. Metallic aluminium, aluminium-alloys, and T-Al (aluminium pre-treated with chloroaluminate melts) have also been proposed. The materials are discussed by type in the following subsections.

3.1.1 Titanium Dioxide

Titanium dioxide (TiO₂) is the most researched and well-established electrode within the aqueous aluminium space thus far. Given this, the elucidation of charge transfer mechanisms is expected to be well known, but it is not. Much research focuses on developing an operational electrode or full battery, reporting performance with a little speculation on the exact mechanisms. Therefore, although this is a well-researched area, there are still many unknowns with regard to the exact charge storage mechanisms. There have been suggestions of

Negative electrodes	electrolytes	Positive electrodes
TiO ₂	AlCl ₃	V ₂ O ₅
MoO ₃	Al(OTF) ₃	FeVO ₄
Al	Al ₂ (SO ₄) ₃	VOPO ₄
Zn-Al	Al(NO ₃) ₃	CuFe(CN) ₆
	Al(CF ₃ SO ₃) ₃	FeFe(CN) ₆
	Al(OTF) ₃	K ₂ CoFe(CN) ₆
		MnO ₂
		Bi ₂ O ₃
		WO ₃

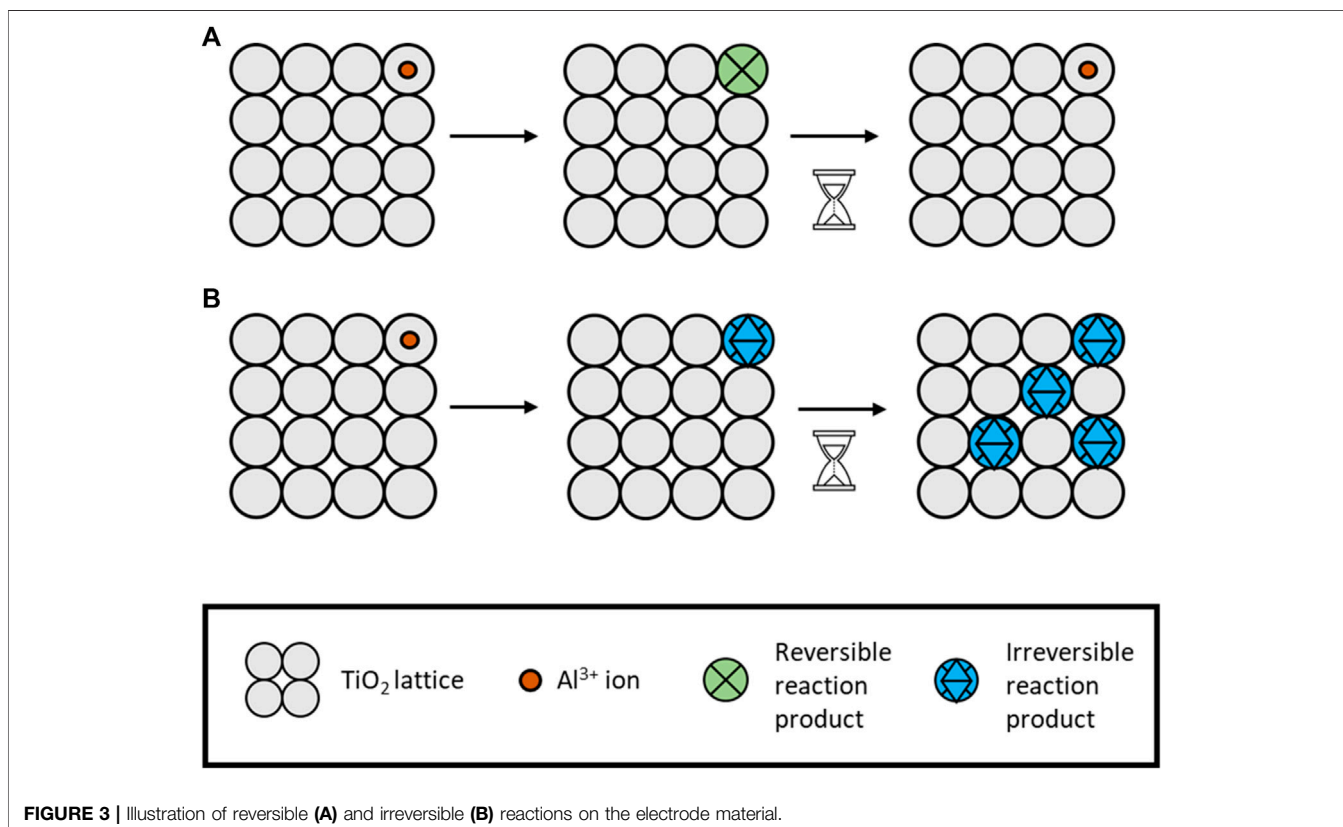
FIGURE 2 | Key materials studied in aqueous Al-ion batteries.

capacitive surface storage, intercalation, and redox reactions using the redox couple Ti³⁺/Ti⁴⁺ (and non-reversible reactions to Ti²⁺).

TiO₂ has been explored as an electrode in other cell designs. However, it was not reported as an option for Al-ion aqueous cells until 2012, at the earliest by Liu et al. (2012). Liu used TiO₂ nanotubes to construct the electrode that the author had previously used for Li-ion aqueous cells (Liu et al., 2011) and

a 1 M AlCl₃ electrolyte. This half-cell was shown to have a specific capacity of 75 mA h g⁻¹ at 4 mA cm⁻², 90% Coulombic efficiency, and a voltage range of 1.1–0.4 V with a discharge plateau between 1.1 and ~0.8 V (Elia et al., 2021; Liu et al., 2012; Holland et al., 2018b). The method of electrochemical exchange is concluded to be the intercalation of Al³⁺ into the TiO₂, with the resulting reaction including Ti-ions (Ti³⁺/Ti⁴⁺) or a non-reversible reaction to Ti²⁺. The author discusses the need for further investigation into the specifics. This is an important aspect for further development. If a non-reversible reaction to Ti²⁺ is occurring, it will reduce the active material available for reactions over time and increase the capacity fade. If the reactions are reversible, then other capacity fade mechanisms may occur, such as lattice structure breakdown. **Figure 3** illustrates these two mechanisms.

Following this, in 2014, further development of the TiO₂ nanotube array was performed, looking at a variety of aqueous Al-ion electrolytes and concentrations (Liu et al., 2014). This study further investigated the role of Ti-ions in the Al³⁺ insertion into the electrode. X-ray photoelectron spectroscopy (XPS) confirmed Al on the surface of the electrode after intercalation but did not find evidence of Cl. More supporting evidence of the Ti³⁺/Ti⁴⁺ role was found, with the author concluding that Ti⁴⁺ must reduce to Ti³⁺ where the Al³⁺ is present on the surface to maintain charge balance. There was also speculation about the additional role of Cl⁻ in the process, confirmed using NaCl as an electrolyte for cyclic voltammetry alongside Al₂(SO₄)₃, which confirmed an assistive role of Cl in the electrochemical reaction



(Liu et al., 2014). Again, much research into the exact reaction mechanisms was clearly needed.

Work on Mg-ion aqueous cells, which produce a divalent ion- Mg^{2+} has also concluded that the redox couple $\text{Ti}^{3+}/\text{Ti}^{4+}$ is involved in the charge storage mechanism (Koketsu et al., 2017). The role of oxygen vacancies within the TiO_2 electrode increases the insertion of the ions, which in turn increases the overall charge storage and capacity.

Holland et al. (2018a) and Holland et al. (2019) further investigated the role of Ti in the charge storage using anatase TiO_2 nanopowder for the basis of the electrode in a 1M AlCl_3 electrolyte. Increasing the pH of the electrolyte with HCl increased the redox peaks seen on a CV (Holland et al., 2018b; Holland, 2018). Initial work suggested that the $\text{Ti}^{3+}/\text{Ti}^{4+}$ reduction only occurs at more negative potentials (~ -1.3 V SCE) and there is some capacitive charge storage at the interface between electrode and electrolyte. This experiment was repeated to further test the capacitive storage hypothesis, using a vacuum impregnation method to construct the TiO_2 nanopowder electrode (Holland et al., 2019). By increasing the contact between the electrode and electrolyte (i.e., using the vacuum impregnation method), Holland et al. found a stable $\sim 100\%$ Coulombic efficiency up to a specific current of 40 A g^{-1} . Compared with the initial work of $\sim 100\%$ Coulombic efficiency up to only 7.2 A g^{-1} (Holland et al., 2018a), this shows the direct impact of increasing contact between the TiO_2 and Al_3Cl , which is convincing evidence for the pseudocapacitive nature at the interface.

The capacitive nature of the charge storage mechanism is further supported by the self-discharge seen in Al-ion aqueous cells with a TiO_2 electrode (Smith et al., 2020). High self-discharge is a trait often seen in capacitors, with batteries and cells often retaining their charge far longer (Afif et al., 2019). Herein, we can find another clue to the pseudocapacitive nature of the charge storage. Given the evidence so far, the primary storage mechanism for Al in TiO_2 is most likely a surface reaction involving the redox pair of $\text{Ti}^{3+}/\text{Ti}^{4+}$ on the surface of the electrode.

Up until this point, the crystal structure of the TiO_2 investigated has been anatase. However, another crystal lattice, rutile, was investigated in 2018 (Tang et al., 2018) as a potential anode material. This computational analysis suggested that the rutile lattice has a far higher diffusion coefficient, D , than that of anatase, $\sim 10^{-9}$ and $10^{-20} \text{ cm}^2 \text{ s}^{-1}$, respectively. In 2019, a rutile nanopowder was studied as an electrode with 1M Al_3Cl electrolyte (Zhao et al., 2019). A solid-phase diffusion of the Al-ions into the TiO_2 was seen. Interestingly, for the rutile electrode, the impedance seen increased with time (cycles), whereas it tends to decrease after the initial electrochemical impedance spectroscopy (EIS) for anatase nanopowders (Tang et al., 2018). There is a need then for different studies to explore the precise mechanism with TiO_2 , considering the crystal structure.

3.1.2 Aluminium and Alloys

The use of Al as the negative electrode is utilised in many ionic-liquid and non-aqueous-based Al-ion systems. Within aqueous

electrolytes, a passivating oxide coating forms on the surface of such an electrode, making the aluminium electrochemically inert. In order to overcome this passivating layer, potentials higher than the ESW would be required, which would degrade the electrolyte itself. When looking at an Al electrode, the key mechanism is the plating and stripping of the metal on the surface of such electrode as it charges and discharges. This is a surface reaction and would theoretically have minimal degradation over time if the passivating layer could be controlled.

Recently, Al anodes treated with chloroaluminate melts have shown reduced amounts of the passivation layer and demonstrated full cells using the treated Al (T-Al) anodes (Zhao et al., 2018; He et al., 2019, Wu C. et al., 2019). Combined with MnO_x cathodes, three key studies in recent years have shown the plating and stripping of aluminium as the mechanism for charge transfer. However, the capacity fade of these cells is high, about 42% after only 65 cycles (He et al., 2019, Wu C. et al., 2019). This indicates that degradation within the electrolyte is still occurring, with the passivating layer still forming over time.

Using a Zn-Al alloy to reduce the passivation layer has been shown by Yan et al. (2020). The Zn seemed to prevent a build-up of a passivating layer, while the Al-ions prevented Zn dendrites from forming. Both the plating and stripping of Al were seen on the surface, as well as an electrostatic/capacitive mechanism.

A recent study looking at Al foil with a KNCHF positive electrode ascribed the capacity fade ($\sim 43\%$ after 500 cycles) to the dissolution of nickel into the electrolyte (Gao et al., 2020). This then reacted with the Al electrode, creating an unstable electrode-electrolyte-interface, which could be seen clearly in XRD and through studying the increase in Ni quantity within the electrode over time. This shows that correct electrode pairing is vitally important in creating a viable Al-ion cell.

3.1.3 Molybdenum Oxides

Molybdenum oxides have also been investigated as a negative electrode. In 2019, Lahan and Shyamal (Lahan and Das, 2019a) investigated the role of electrolytes in the performance of MoO_3 . They concluded that 1 M AlCl_3 was the superior electrolyte and found an impressive initial discharge capacity of 680 mA h g^{-1} at 2.5 A g^{-1} . However, by the 20th cycle, this had dropped considerably to 168 mA h g^{-1} . This then remained stable up to 350 cycles, with no sign of further decaying. This phenomenon was explained by the initial 'trapping' of the intercalating Al^{3+} in the MoO_3 structure over the first cycles, an irreversible process occurring alongside the reversible one. Interestingly, in 1 M $\text{Al}(\text{NO}_3)_3$, the authors found an initial discharge of $21,296 \text{ mA h g}^{-1}$ at 2.5 A g^{-1} , which then decayed to 15 mA h g^{-1} by the 15th cycle. Again, the high initial discharge capacity indicates irreversible side reactions, such as corrosion, which damaged the electrode, leading to the lower stabilised capacity of 15 mA h g^{-1} .

Later work in 2019 and 2020 by Wang et al. (2019), Wang et al. (2020), however, found that 1 M $\text{Al}(\text{NO}_3)_3$ was a suitable electrolyte using MoO_3 nanobelts as the electrode material. The two studies show similar CV profiles for this setup and also concur with the profiles reported by Lahan and Das (2019a).

Galvanostatic curves were collected for Wang et al. (2019) and Wang et al. (2020), with Wang et al. (2020) showing a more 'expected' profile and initial discharge of $\sim 308\text{--}232\text{ mA h g}^{-1}$ at $1\text{--}8\text{ A g}^{-1}$, two orders of magnitude fewer than those by Lahan and Das (2019a) suggesting that the side reactions were reduced with the nanobelt structure. The profiles shown by Wang et al. (2019) are for MoO_3 with a polypyrrole (Ppy) coating and show lower capacities.

There are no cycling data provided for this half-cell setup to compare. However, Wang et al. (2020) used MoO_3 to create flexible solid-state cells with a gelatin-PAM electrolyte with $1\text{ M Al}(\text{NO}_3)_3$, which performed 2,800 cycles with only 13.8% capacity fade seen. The low-capacity fade is another indicator that there were fewer side reactions. The storage mechanisms were discussed in terms of the nanobelt structure and crystallographic plane of the MoO_3 (010), favourable for ion intercalation. XRD also showed that the d-spacing increased with Al^{3+} insertion but went back to the pristine spacing on extraction, implying no permanent structural changes within the electrode, which may explain the long cycle life (Wang et al., 2020). Further work introducing tantalum to the MoO_x and creating a nanotube array electrode also suggests long cycle life (3,000 cycles with 17% capacity fade) (Jin B. et al., 2021).

3.2 Positive Electrode

The positive electrode, for secondary cells, is the material that has a higher potential when in a full cell. **Supplementary Table S2** summarises the materials that have, to date, been studied as positive electrodes for an aqueous aluminium-ion cell. As with the previous section, half and full cell data are listed.

3.2.1 Vanadium Containing Electrodes

Vanadium oxides have been explored as cathodes or positive electrodes in various metal-ion cells (Song et al., 2018). More recently, aqueous Zn-ion cells have shown promise with a V_2O_5 electrode (Javed et al., 2020).

Vanadium pentoxide xerogel (xero- V_2O_5) was first studied in aqueous Al-ion cells in 2016 (González et al., 2016). Using an electrolyte of 1 M AlCl_3 , it was shown that a discharge capacity of 120 mA h g^{-1} at 60 mA g^{-1} could be achieved. With increasing current densities, however, the performance suffered 20 mA h g^{-1} at 200 mA g^{-1} . This suggests that the reaction at the electrode is diffusion controlled. The authors suggest that both protons and Al-ions intercalate into the electrode simultaneously during discharge. It is already known that, within the interlayers of xero- V_2O_5 , protonated water and charged ions (such as Al^{3+}) can be easily exchanged when in an aqueous media (Znaidi et al., 1989). Therefore, the ion exchange process may be happening alongside the intercalation. During charging, this ion exchange may trap the Al-ions within the electrode structure and reduce the overall available capacity. This may be a reason for the high fade seen ($\sim 38\%$) after only 12 cycles (González et al., 2016). Further, the intercalation of protons from the water can reduce vanadium oxide, limiting the discharge capacity.

Kumar et al. (2019) investigated FeVO_4 as a cathode material, again with an electrolyte of 1 M AlCl_3 . However, in this study, ammonium hydroxide was added to the electrolyte to increase the

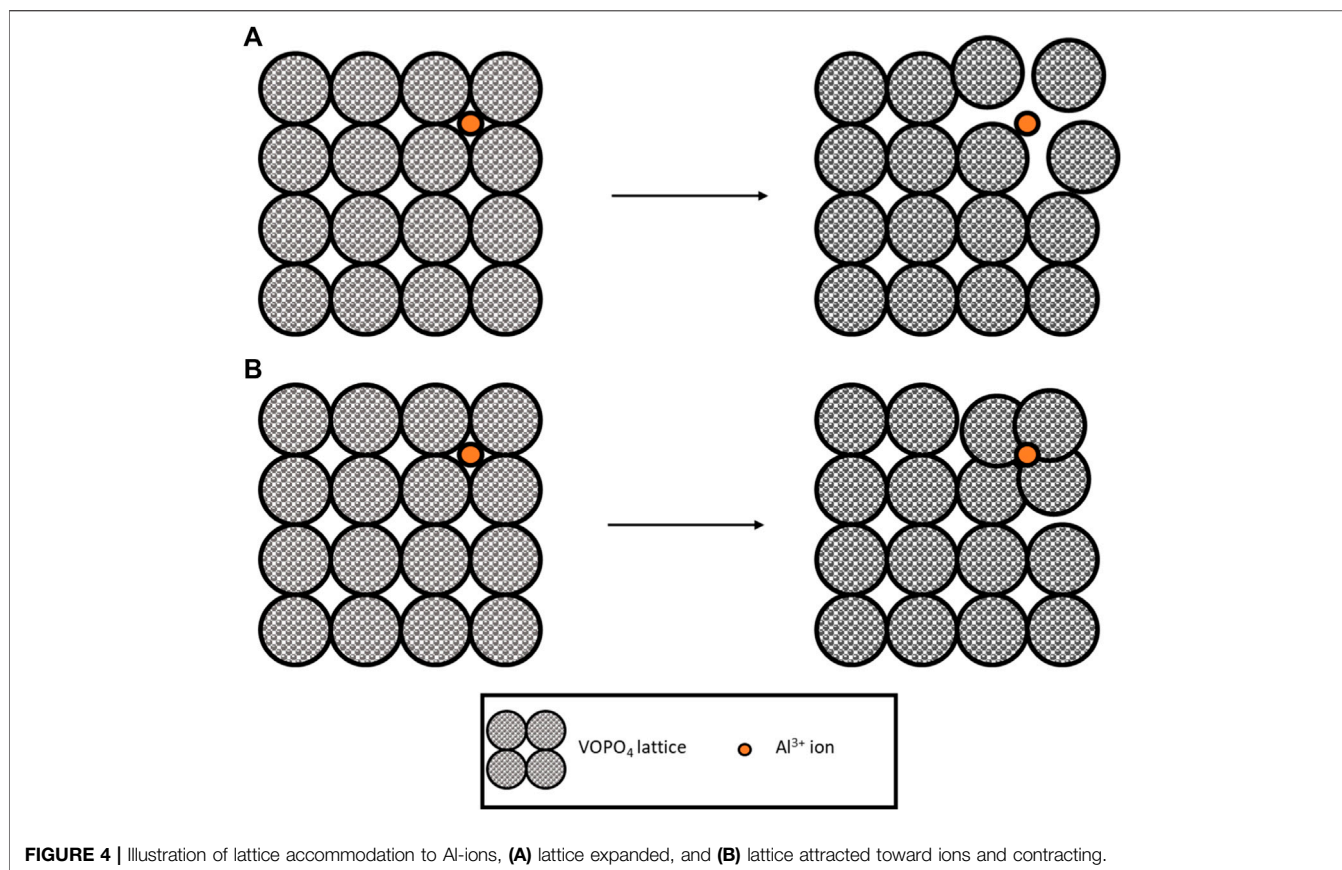
pH to 3.5. The increased pH showed a high specific capacity of 350 mA h g^{-1} at 60 mA g^{-1} . Initial conclusions from this study were that aluminium was reacting reversibly with the cathode. However, the exact mechanisms were complex. The study concluded that there were reactions between the cathode and Al^{3+} and with the electrolyte itself. The rapid fading of this cell of 85% after 20 cycles is indicative of the parasitic reaction of the cathode with the electrolyte: loss of vanadium as V^{5+} to the electrolyte. These reactions also show a phase change of the cathode material, from a triclinic lattice to a more symmetrical system. There is some speculation about the reversibility of this change. Overall, the need for an EEI (electrode-electrolyte interface) layer is discussed to reduce the parasitic reaction and maintain the high specific capacities found.

More recently, bronze-type vanadium dioxide holey nanobelts ($\text{B-V}_2\text{O}_5$) have been studied as a positive electrode. The nanobelts act like layers, and the holey nature increases the surface area of the electrode, allowing easier, shorter diffusion paths for the Al-ions. When investigated in a $5\text{ M Al}(\text{TOF})_3$ electrolyte, a high capacity of 234 mA h g^{-1} at 150 mA g^{-1} was seen and, at higher current densities (1 A g^{-1}), achieved 1,000 cycles with 22.8% fade. Initially, the discharge capacity rose between cycles. This initial rise could be due to the electrolyte taking time to soak into all the electrode pores or irreversible reactions taking place. The key reaction mechanism discussed was the parallel intercalation of Al^{3+} and H^+ into the $\text{B-V}_2\text{O}_5$ because of the hydrated Al-ions within the aqueous electrolyte. This is a similar mechanism as suggested for the xero- V_2O_5 (González et al., 2016). Additionally, the reduction of V^{4+} to V^{3+} is seen alongside the intercalation. Similar to Kumar et al. (2019), some vanadium (as V^{5+}) is also seen to dissolve into the electrolyte in the initial cycles.

Further evidence of vanadium dissolution into the electrolyte was found by Zhao et al. (2020) with a V_2O_5 nanorod cathode. The same fast decaying capacity over cycles was observed and attributed again to the vanadium dissolving into the $2\text{ M Al}(\text{OTF})_3$ electrolyte. The capacity faded from 186 to 20 mA h g^{-1} at 40 mA g^{-1} after fifty cycles. A barrier layer of Nafion was then placed on the surface of the electrode to minimise the movement of vanadium into the electrolyte. While the charge/discharge profiles were comparable to the unprotected electrode, the capacity fade was much improved. After 50 cycles, the discharge capacity was still $\sim 120\text{ mA h g}^{-1}$ at 40 mA g^{-1} .

In terms of the charge storage, analysis of SEM and EDX data showed that the aluminium may not have been intercalating into the electrode during discharge but forming a soluble product on the surface of the V_2O_5 . Due to the lower pH of this electrolyte (~ 2), it was reasonably assumed that H^+ was more likely intercalating into the V_2O_5 with fewer Al^{3+} . This compares well with Kumar et al. (2019), who saw an increase in cell capacity at higher electrolyte pH, and other vanadium studies, which see the proton intercalation occurring alongside Al^{3+} (González et al., 2016; Cai et al., 2020).

In 2020, a flexible hydrogel electrolyte was used with a VOPO_4 electrode to create a flexible battery (Wang et al., 2020). The long cycle life of this battery (2,800 cycles at 1 A g^{-1}) and low-capacity fade ($\sim 13.8\%$) shows promise for aqueous gel electrolytes



combined with vanadium-containing electrodes. The study did not mention any vanadium dissolution into the electrolyte. Due to the long cycle life, it seems reasonable that this was not present. However, a more recent study of VOPO_4 in $\text{Al}(\text{CF}_3\text{SO}_3)_3$ showed a 40% fade after only 40 cycles (Pang et al., 2021). The key charge transfer mechanism was identified as the intercalation of Al^{3+} combined with the redox pairs $\text{V}^{5+}/\text{V}^{4+}$ and $\text{V}^{4+}/\text{V}^{3+}$. Interestingly on intercalation, the d-spacing (distance between layers in a crystal lattice) between VOPO_4 layers decreased when accommodating the Al^{3+} . Usually, the interlayers have been shown to increase as the Al^{3+} distorts the lattice to ‘fit’ in **Figure 4A**. However, in this case, the electrostatic charge of the Al^{3+} must attract the negative oxygen atoms in the lattice (**Figure 4B**). This process was confirmed as reversible, with the d spacing returning to pristine condition on deintercalation.

3.2.2 Prussian Blue Analogues

Prussian blue analogues (PBAs) have the structure $A_xM\text{Fe}(\text{CN})_6$, where A is an alkali metal or alkaline Earth metal and M is a transition metal. PBAs have open lattice frameworks characterised by large ionic channels and interstitial sites. These properties make them good candidates for electrode materials as they can accommodate guest ions within the framework easily. PBAs have been investigated as electrodes for other multivalent ions (Chen et al., 2017; Gheyhani et al., 2017; Kong et al., 2014; Wessells et al., 2011).

Copper hexacyanoferrate ($\text{KCuFe}(\text{CN})_6$, more commonly abbreviated as CuHCF) was investigated in an electrolyte of 1 M AlCl_3 + 1 M KCl (Holland et al., 2018b; Holland et al., 2018c). The presence of Fe in the electrolyte after cycling suggested an irreversible displacement of the Fe from the electrode within the cell. No further spectra or chemical analyses were performed on the electrode sample. Therefore, it is difficult to understand the exact reaction. The Al^{3+} and K^+ ions may have contributed to this displacement during cycling. CuHCF has been used in K-ion cells, citing the intercalation of K^+ alongside the reduction of Fe^{3+} to Fe^{2+} (Xia et al., 2020; Jiang et al., 2019). In 2019, Wang et al. (2019) investigated a flexible Al-ion cell with a CuHCF positive electrode and MoO_3 negative electrode (this work precedes Wang et al., 2020). Prior to building the cell, Al^{3+} was pre-inserted into the CuHCF electrode. During discharge, a reduction of Fe^{3+} to Fe^{2+} was observed, maintaining the charge balance of the electrode as the Al-ions were extracted. Unlike Holland et al. (2018c), there was no mention of the loss of Fe to the electrolyte. Wang et al. used only an aluminium salt electrolyte, unlike Holland et al., who used both Al and K salts. The exact mechanism which led to Fe displacement requires further investigation.

Potassium cobalt hexacyanoferrate ($\text{K}_2\text{CoFe}(\text{CN})_6$) nanocubes have also been studied as a positive electrode in 1 M $\text{Al}(\text{NO}_3)_3$ (Ru et al., 2020). Here, the charge mechanism was identified as Al^{3+} intercalation into vacant potassium sites within the cubic lattice of the electrode. The corresponding reactions at the

electrode to maintain balance are $\text{Fe}^{3+}/\text{Fe}^{2+}$, typical of all PBAs so far. A second peak in the CV corresponding to the pair $\text{Co}^{2+}/\text{Co}^{3+}$ was also identified. A two-step reaction is therefore possible with a 'dehydration step' involved prior to insertion into the lattice. The cycling performance is investigated, with 1,600 cycles performed, with a 25% capacity fade. Through SEM, it was shown that the nanocubic framework had partially collapsed after 1,600 cycles, suggesting that structural changes due to cycling cause capacity decay. The decay may be caused by the large charge density of the Al^{3+} distorting the structure or the physical size of the ion replacing the K vacancies due to Al's larger ionic radius. Of further interest, this electrode was examined with other electrolyte salts (AlCl_3 and $\text{Al}_2(\text{SO}_4)_2$), and the performance was superior with $\text{Al}(\text{NO}_3)_3$. This makes the clear argument that it is not just the choice of the electrode but the appropriate electrolyte that can impact the performance and overall electrochemical mechanisms involved.

Water-in-salt electrolytes (WISE) describe an electrolyte whereby the salt outnumbers the water (solvent) in volume and weight (Suo et al., 2015). When this occurs, the water molecules do not fully solvate ions, and thus there are interionic pairs. This greatly increases the ionic conductivity and increases the ESW for the electrolyte (Suo et al., 2017). Using this approach, a WISE was created with 5 M $\text{Al}(\text{OTF})_3$ to investigate $\text{FeFe}(\text{CN})_6$ (chemical equation $\text{K}_{0.2}\text{Fe}[\text{Fe}(\text{CN})_6]_{0.79}\cdot 2.1\text{H}_2\text{O}$) as an electrode material (Zhou et al., 2019). The ESW was increased from 1.23 to 2.65 V, which facilitated a high specific capacity of 116 mA h g^{-1} at 150 mA g^{-1} , the highest seen for PBA electrodes currently. The reaction mechanisms within this system are discussed extensively. On initial charges, the cell capacity slowly increases due to the removal of residual K-ions over the first few cycles (providing more vacancies for Al^{3+} on subsequent cycles). Additionally, within the first few cycles, irreversible structural changes of the electrode lattice are seen from XRD, which may decrease but also stabilise the overall capacity by 'trapping' some Al-ions.

The redox pair $\text{Fe}^{3+}/\text{Fe}^{2+}$ was observed, as is expected for PBAs, alongside Al^{3+} intercalation. There is also speculation about the role of K^+ , as well as protons within the charge/discharge process. However, further studies are needed to understand these interactions. Further, the authors claim 'good cycling stability' (Zhou et al., 2019). Far superior PBA cycling stability has been observed in CuHCF discussed above (Holland et al., 2018b; Holland et al., 2018c; Liu et al., 2015).

Although not described as a WISE, a high concentration (5 M $\text{Al}(\text{CF}_3\text{SO}_3)_5$) was the electrolyte used with a potassium nickel hexacyanoferrate (KNHCF) electrode to make a cell with an Al foil negative electrode (Gao et al., 2020). Again, the redox pair $\text{Fe}^{3+}/\text{Fe}^{2+}$ was observed, alongside $\text{Ni}^{3+}/\text{Ni}^{2+}$, during reversible Al^{3+} intercalation similar to that shown by Ru et al. with the $\text{Co}^{2+}/\text{Co}^3$ pair in the two-step reaction. A similar process may occur herein. The KNHCF structure remained unchanged after 500 cycles, which suggests a stable positive electrode material for aqueous aluminium cells. Unfortunately, the capacity fade seems primarily due to the Al foil as aluminum corrodes readily in an aqueous environment. It would be useful to see KNHCF studied

with different counter electrodes or with TiO_2 as the negative electrode to fully see the limits of this material.

3.2.3 Manganese Oxides

In the last few years, manganese oxides have been researched as electrodes, both when combined as an Mn-Al ion battery (Zhao et al., 2018; He et al., 2019) and with only Al-ions as the charge carrier.

A multi-step process has been identified by a few studies, whereby Mn^{2+} initially dissolves into the electrolyte on the first discharge, forming an amorphous on the surface at the first charge. This layer is likely composed of Al, Mn, and O and is likely soluble in water. Then, this layer 'plates and strips' in subsequent cycles. Adding Mn salt initially into the electrolyte enhances the overall performance. These cells can therefore be described as Mn-Al ion cells.

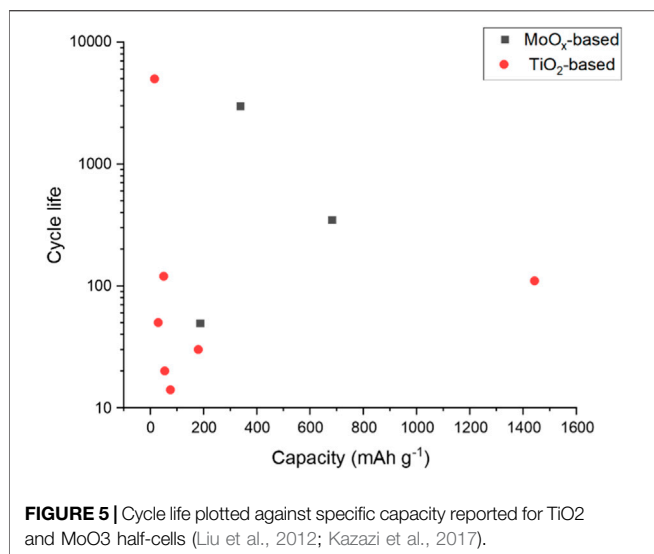
When looking at the nanostructures, nanorods and nanowires have been investigated by Joseph et al. (2019a) and Joseph et al., (2020). Potassium-rich manganese oxide was investigated, which formed nanowires in 1 M $\text{Al}(\text{NO}_3)_3$. During charge, there was a switch between the K and Al, whereby K-ions would dissolve into the electrolyte and be replaced by Al^{3+} in the vacancies. Over time, the K-ions did not re-insert and the concentration of K in the electrolyte increased as cycling continued (Joseph et al., 2019b). When researching the magnesium doped MnO_2 nanorods, a similar mechanism was reported whereby the Mg^{2+} ions create large tunnels in the structure, which allow for easy Al^{3+} intercalation (Joseph et al., 2020). There is some speculation on whether this is a similar 'exchange' as shown by Joseph et al. (2019a). Additionally, to the intercalation, there is some capacitive charge storage observed at the surface of the electrode.

A mixture of surface mechanisms such as forming a new layer or capacitive storage is observed along with intercalation of Al^{3+} in the bulk of the electrode. If both surface and bulk processes can be taken advantage of and optimised, this may be an exciting material for high-performance Al-ion aqueous battery research.

3.2.4 Other Materials

The use of graphite is more common in non-aqueous Al-ion batteries. However, two studies have recently used them as the positive electrode within an aqueous cell (Mohanapriya and Jha, 2019; Nandi et al., 2019). Multi-layer graphite (as discussed in Nandiet al., 2019) showed an intercalation/deintercalation of Al^{3+} between layers. However, the expansion of the lattice during insertion led to cracking of the structure and hence a short cycle life. However, when looking at graphene with the addition of carbon nanoparticles, a capacitive storage mechanism is suggested, which may lead to longer cycle life (apparently 0% fade over 3,500 cycles; Mohanapriya and Jha, 2019), but potentially a higher self-discharge.

Bismuth oxide (Bi_2O_3) was investigated in 2020 by Nandi and Shayamal (Nandi and Das, 2020). Initial discharge capacities in a full cell with Al-ion negative electrode showed very high values ($1,130 \text{ mA h g}^{-1}$ at 1.5 A g^{-1}) and ~99% Coulombic efficiency. However, this dropped significantly to 103 mA h g^{-1} within 20 cycles and remained stable for the following 50 cycles, showing no



additional signs of capacity fade. This behaviour suggests that more complex reactions are set up in the initial cycles, with potential parasitic reactions, which require further investigation, suggesting an alloying reaction between Bi and Al and interfacial storage between Bi and Al₂O₃ at the electrode/electrolyte interface.

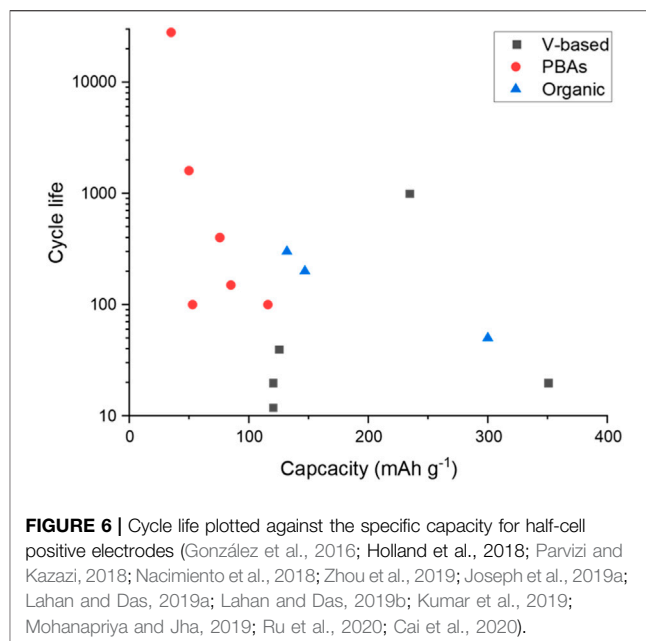
Although WO₃ electrodes show poor Coulombic efficiency [~80% (Lahan and Das, 2019b)] over cycling in both 1 M AlCl₃ and 0.5 M Al₂(SO₄)₃, the capacity increases over cycling time to around double the initial capacity seen. With no significant structural changes seen in the electrode after 100 cycles and the main mechanism assumed to be intercalation/deintercalation of Al³⁺, this could be an interesting material to study if the Coulombic efficiency can be improved.

In the last year, organic materials have been studied as electrodes, with quinones (Li et al., 2021; He et al., 2021) studied as positive (as well as negative; Yan et al., 2021) electrodes and phenazines (Chen et al., 2021). These electrodes see conversions between hydroxyl and carbonyl groups, alongside the insertion/extraction of Al³⁺.

3.3 A Note on Half-Cells

Overall, the negative electrode half-cells reported in the literature can be summarised as TiO₂-based or MoO₃-based. **Figure 2** plots the reported cycle life of these half-cells against the specific reported capacity. While the current density is not shown in this plot, we can see a cluster of low specific capacity reported for TiO₂-based half-cells. Two MoO₃ based half-cells are reported with sufficient data to plot. However, a trend in higher specific capacity may be achievable with this electrode basis.

All but one of the reported half-cells have a cycle life above 350. TiO₂ anatase nanopowder, with 1 M AlCl₃ + 1 M KCl electrolyte, shows excellent cycle life of 5,000 cycles (Holland et al., 2018a). Other TiO₂-based electrodes only use an aluminium salt in the electrolyte and do not have an additional potassium salt. Therefore, there may be potential in exploring electrolyte additives to improve the cycle life.



There are many half-cells reported in the literature for the positive electrode. **Figure 5** plots the cycle life against the specific capacity for half-cells with both these values reported in the literature. From the limited dataset provided, there is a suggestion that higher specific capacities (above 200 mA hg⁻¹) are achievable using vanadium-based electrodes. Although the highest capacity example only reported a cycle life of 20 cycles. One data point for the graphite-based electrode does not provide a pattern. However, the capacity reported that 157 mA hg⁻¹, along with a promising cycle life of 3,500 cycles, would suggest further investigation into this electrode design (Mohanapriya and Jha, 2019). Interestingly, the highest reported cycle life is with the lowest specific capacity. Although all the PBAs appear to have a lower specific capacity, anomalous 28,000 cycles are reported for a CuHCF based electrode (Holland et al., 2018c). As with the high cycle life TiO₂ from the negative electrode example, this electrode was tested in an electrolyte with both aluminium and potassium salts, suggesting that the potassium may help with cycle life extension but perhaps not increase capacity.

Figure 6 plots the potential ranges for a selection of half-cells. Most negative electrodes (TiO₂ based) that report potential ranges are between -1.2 and -0.8 V vs. Ag/AgCl. For the positive electrodes, there is more variation in the potential range. Already pairs of electrodes for full cells can be suggested; TiO₂ and CuHCF make an obvious pairing and have been studied extensively by Holland et al. (2018b) and Holland (2018). **Figure 7** shows that this cell, with AlCl₃ + KCl electrolyte, has a low capacity but long cycle life compared to other combinations (apart from MoO₃//VOPO₄). A potential combination that has not been discussed in the literature may be TiO₂ and MnO₂ electrodes, as they have a large potential range between them. So far, MnO₂ has only been studied with

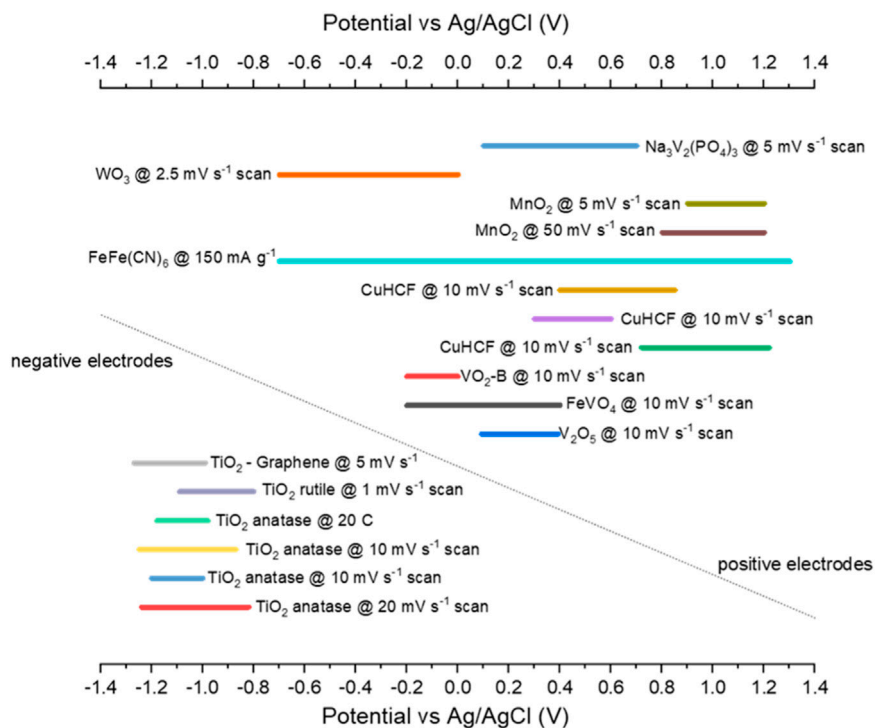


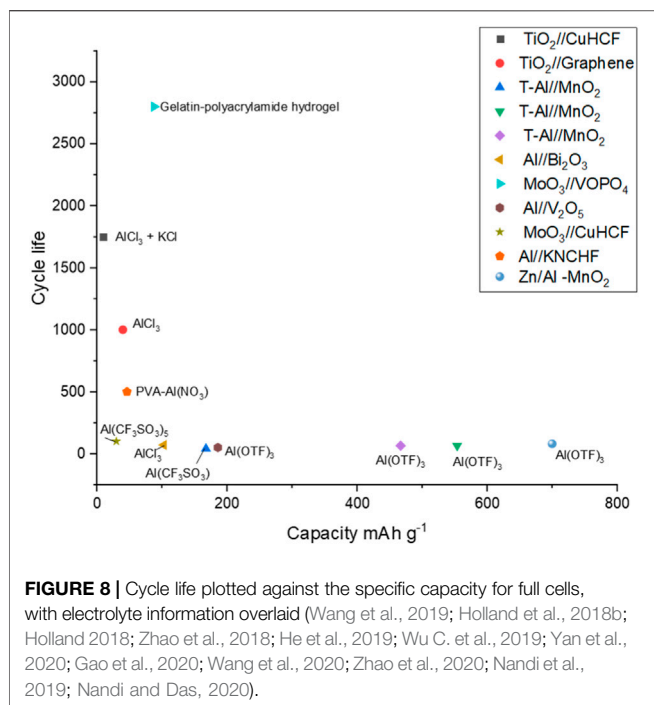
FIGURE 7 | Potential ranges reported for various half-cells converted to Ag/AgCl (Liu et al., 2012; Liu et al., 2014; Holland et al., 2018a; Holland et al., 2019; Holland, 2018; Zhao et al., 2019; Kumar et al., 2019; Zhao et al., 2020; Cai et al., 2020; Holland et al., 2018c; Zhou et al., 2019; Liu et al., 2015; Joseph et al., 2019; Joseph et al., 2020; Lahan and Das, 2019b; Lahan et al., 2017; Nacimiento et al., 2018).

Al electrodes, which could be argued as half-cells with an Al counter electrode, as opposed to full cell studies. Therefore, combining MnO₂ with TiO₂ in a full cell would be useful.

3.4 Full Cells

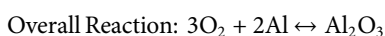
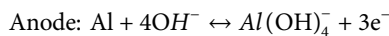
As stressed throughout this review, understanding how electrodes behave like a full cell is important for the potential commercialisation of aqueous Al-ion technology. **Figure 8** plots the cycle life against the specific capacity reported for full cells in the literature. The electrolyte used is overlaid, with cells grouped in rectangles that share a common electrolyte component. It could be suggested that full cells with an Al electrode, whether alloyed with Zn or pre-treated, have low cycle life regardless of the electrolyte. This can be seen with AlCl₃, Al(CF₃SO₃), and Al(OTF)₃, all showing low cycle life when paired with an Al electrode in a full cell. This is most likely due to the passivating layer, which forms on the Al in the cell, which in half-cells may not have been such a limiting factor. Further, Al foil is often not used as an electrode in a full cell but rather as the counter electrode in a half-cell setup. The authors discuss their work as full cells and as such they have been reported as full cells in this review, an Al electrode in a secondary aqueous cell is not likely to be practical or developed commercially. A case could be made that the Al(OTF)₃ also leads to lower cycle life cells. Because all reported examples have an Al-based electrode, much research into this electrolyte may be useful. The AlCl₃ electrolyte appears to give good cycle life for TiO₂ containing

electrodes with the addition of KCl increasing cycle life further, although not to the same extent as the half-cells. Hydrogel electrolytes appear to increase cycle life substantially with the PVA-Al(NO₃)₃ electrolyte combined with the aluminium and PBA electrodes providing just over 500 cycles (Wang et al., 2019)—the highest reported for an Al-containing electrode within a full cell. Clearly, the gelatin-polyacrylamide hydrogel has the highest cycle life reported for a full cell, 2,800, with a 13.8% capacity fade (Wang et al., 2020). Half-cell vanadium-containing electrodes reported between 12 and 1,000 cycles (González et al., 2016; Kumar et al., 2019; Cai et al., 2020), while half-cell MoO₃ (Lahan and Das, 2019b; Joseph et al., 2019b) electrodes had cycle lives of 350–400. This hydrogel result requires much research, as this increase in cycle life combined with the flexibility of the cell described would certainly show commercial potential. Overall, **Figure 8** demonstrates that there is no middle-ground currently with respect to capacity and cycle life; either high capacity or high cycle life is demonstrated, but both are unlikely, given the location of examples close to the axes. This then asks the development question, do we look to high capacity and attempt to increase cycle life or look to high cycle life and attempt to increase capacity? Do the cells with high cycle life demonstrate a pseudocapacitive storage mechanism, which may enable longer life and less damage to the electrodes? These research questions need further study and understanding.



4 AL-AIR AND PRIMARY BATTERIES

Aqueous aluminium-air batteries are generally non-rechargeable, primary batteries. Unlike supercapacitors or most secondary batteries, the ions within the electrolyte are not the charge carriers of the reaction. The main charge transfer mechanism is the reduction of oxygen from the air at the cathode combined with the oxidation of the aluminium-containing anode. The reaction is often reported as follows:



Corrosion of the anode, or a build-up of a passivation layer, often limits the capacity and lifetime of an Al-air battery. This section will discuss development in minimising corrosion and increasing utilisation at the anode. Additionally, the oxygen reduction reaction (ORR) at the cathode is a prime source of research, with electrocatalyst chemistries studied to speed up this reaction.

Supplementary Table S3 summarises some of the aqueous Al-air studies from recent years. However, unlike with secondary batteries (where there are common data provided within the majority of research), the data provided within these studies vary. Therefore there are a few holes within **Supplementary Table S3**. These holes certainly point to future potential studies to acquire more data and more comparable data to fully understand the performance of these cells. However, this is a complaint often found when reviewing papers as different researchers wish to optimise different performance parameters.

4.1 Anodes

As previously mentioned, all anodes for Al-air batteries contain aluminium. This ranges from high purity Al (Di Palma et al., 2017; Gaelle et al., 2021; Teabnamang et al., 2020; Xue et al., 2017; Hopkins et al., 2018) to complex lab-created alloys (Wanget al., 2017; Pino et al., 2016; Zhang et al., 2019, Wu Z. et al., 2019) as well as the use of commercial off the shelf (COTS) alloys (Katsoufiset al., 2020; Ryu et al., 2018; Mutlu et al., 2017).

High purity Al anodes are often used when investigating the impacts of a cathode, catalyst, or electrolyte additive and, therefore, will not be discussed further in the section. The high purity Al is seen as the 'baseline'. By manipulating the anode, it has been shown that the potential can be changed (Wang et al., 2017), which increases the ESW, corrosion and side reactions can be limited, and anode utilisation can be increased (Pino et al., 2016).

The addition of antimony (Sb) to create an Al-alloy has been studied on various occasions, with the conclusion that the Al-Sb precipitates can inhibit corrosion of the anode and slow down the growth of a passivation layer on the anode surface (Zhang et al., 2019; Liu et al., 2019, Zhang P. et al., 2020; Liu X. et al., 2020). These anodes also showed a high OCV of >1.80 V, indicating that HER may be reduced due to the increased ESW of the electrodes.

Coating the anode has also been researched to inhibit any passivation layers that may grow and allow increased utilisation of the anode. Carbon black was investigated as a coating on two Al alloys: Al1085, a high purity alloy, and Al7475, which contains Zn, Mg, Si, and Cr. As expected, the coating on the anodes increased the anode utilisation and cell capacity compared to the non-coated counterparts, with the coated Al745 achieving double the specific capacity of the uncoated Al7475 (540 and 1,210 at 10 mA cm⁻², respectively) (Pino et al., 2016).

4.2 Cathodes and Catalysts

Platinum and manganese oxide catalysts are commercially available and well established in Al-air cells. They are often used in studies investigating the electrolyte or anode specifically and will not be discussed in this section.

There have been few studies on new catalyst materials in the last five years. However, in 2018, Wang et al. (2018) investigated the use of a Fe-N-C catalyst and found it to comparable in performance to Pt/C and an open-circuit voltage OCV of 1.74 V, which is relatively high for these batteries. The key advantage discussed here is the cost-effectiveness and ease of production of Fe-N-C compared to Pt. A follow-up study in 2019 substituted some Cu for Fe (Li et al., 2019) and found that the ORR was further boosted with this substitution.

Catalysts are primarily attached to a cathode substrate, such as a mesh or foam (normally nickel), with the use of binders. In 2020, a study looked at binder-free cathodes using Co₃O₄ nanosheets (Liu et al., 2020).

4.3 Additives and Electrolytes

Liquid aqueous electrolytes typically used in Al-air cells are KOH, NaOH, and NaCl, with limited discussion on the reasoning behind this choice in a particular battery.

Adding different additives to electrolytes to inhibit anode corrosion is of particular interest. K_2SnO_3 and APG were studied in 4 M KOH with an Al alloy anode and $MnxOy/Ag$ cathode catalyst (Wu et al., 2020). The addition of the corrosion inhibitors allowed a uniform protective layer to form from the Sn within the Al alloy, compared to the uneven and rough layer formed without these additives. This layer protected the anode from corrosion and increased the capacity seen. The final reported capacity was 2,180 mA h g⁻¹ at 100 mA cm⁻². However, which additives are used in electrolytes is not always fully reported. For example, 'corrosion inhibitors' were added to 6 M KOH by Wang et al. (2018), but their name and effect were not commented on.

More recently, hydrogels have been explored as electrolytes, particularly in a dual-electrolyte system. Using a hydrogel as a catholyte and a non-aqueous anolyte (Teabnamang et al., 2020) reduces corrosion at the anode, increasing its utilisation. A 40 h discharge was reported for this cell at a current density of 10 mA cm⁻². The capacity reported was also comparable to other Al-air cells (2,328 mA h g⁻¹). Gaele et al. (2021), using a similar approach to the electrolytes, had a very low reported (50 μ Ah g⁻¹ at 100 μ A cm⁻²) capacity. These two studies are not fully comparable, as they used different cathodes, catalysts, catholytes, and anolytes in their designs, showing that there is potential in dual electrolyte technology. However, there are now more variables to assess and presumably more trial and error to come.

5 AL-IONS IN AQUEOUS SUPERCAPACITORS

Energy storage in capacitors is achieved due to charge separation, and in more typical supercapacitors, this is due to the electrochemical double-layer capacitance (EDLC). Additionally, in what would be called a pseudocapacitor (or capattery or cabattery), a mix of EDLC and surface adsorption or redox reactions can be seen (Afif et al., 2019). The primary charge storage of these devices is charge separation.

Supercapacitors traditionally have longer cycle life than batteries, as the electrochemistry does not occur within the electrode and, therefore, the structural changes seen in batteries are unlikely in supercapacitors. This can be seen with 10,000 cycles performed and around 10% fade in capacitance (Tian et al., 2019; Krishnamoorthy and Jha, 2019). **Table 2** summarises recent Al-ion aqueous supercapacitors.

In recent years, only a few aqueous Al-ion supercapacitors have been investigated. However, for batteries, TiO_2 (Holland et al., 2018), and graphite (Mohanapriya and Jha, 2019), capacitive storage has been identified as one of the storage mechanisms. With both these materials researched as supercapacitor electrodes (Krishnamoorthy and Jha, 2019; Zhong et al., 2015), Krishnamoorthy and Jha (2019) suggested using their electrode as a cathode for an Al-ion battery before demonstrating its use in a supercapacitor with an ionic liquid. Therefore, it is useful to consider the potential

for Al-ion use as a hybrid capacitor, which could reduce the cost and complexity of these applications (Smith et al., 2020).

6 CONCLUSION

Aluminium can be a major player in energy storage solutions. Its high volumetric energy density, 8.04 Ah cm⁻³, abundance, pre-existing production industry, and recyclability make it a sustainable option. Pairing this technology with aqueous electrolytes in batteries and supercapacitors can produce inherently safe and cheap energy storage. The versatility of these systems has been discussed in the review.

Primary aluminium-air batteries are the most developed technology, with work toward increasing anode utilisation and reducing side reactions ongoing. The capability for rechargeable aqueous Al-air batteries is only just investigated, so there is the opportunity to develop this further.

Secondary Al-ion batteries have increased attention in the last 5 years, with the exact charge storage mechanisms remaining complex and unknown for many electrodes. This is clearly a space with the potential for growth, with the better elucidation of reaction mechanisms and refinement of electrode choice. Al-ions have various charge transfer mechanisms. For the TiO_2 negative electrodes, a surface pseudocapacitive reaction is most likely, while lattice expansion due to Al^{3+} insertion in vanadium-containing positive electrodes shows that bulk reactions are also possible. There are still many unknowns regarding the charge transfer within many electrode materials, with an engineering focus primarily on 'does it work' prior to the investigation into how. This is illustrated for CuHCF electrodes with as yet unexplained displaced Fe in the electrolyte. There are few studies into supercapacitors with Al-ion technology. However, many of the secondary batteries have pseudo-capacitive behaviour. It is expected that, as the exact charge storage for some electrodes (such as TiO_2) is determined, the role of Al-ion technology may shift toward supercapacitor storage.

AUTHOR CONTRIBUTIONS

NM: research and writing. RGAW: editing, support, and writing.

FUNDING

This work was funded by UKRI under an STFC Studentship and the EPSRC Faraday Training Grant EP/S514901/1, CN7961 S3 2020 001.

SUPPLEMENTARY MATERIAL

The Supplementary Material for this article can be found online at: <https://www.frontiersin.org/articles/10.3389/fceng.2022.778265/full#supplementary-material>

REFERENCES

- Afif, A., Rahman, S. M., Tasfiah Azad, A., Zaini, J., Islam, M. A., and Azad, A. K. (2019). Advanced Materials and Technologies for Hybrid Supercapacitors for Energy Storage - A Review. *J. Energy Storage* 25, 100852. doi:10.1016/j.est.2019.100852
- Ai, Y. (2020). A High-Capacity Aqueous Rechargeable Supercapacitors Based on Electrochemical Al³⁺ Intercalation. *Meat. Abstr.* 02, 1994. doi:10.1149/ma2020-02291994mtgabs
- Bai, R., Yang, J., Li, G., Luo, J., and Tang, W. (2021). Rechargeable Aqueous aluminum-FeFe(CN)₆ Battery with Artificial Interphase through Deep Eutectic Solution. *Energy Storage Mater.* 41, 41–50. doi:10.1016/j.ensm.2021.05.025
- Butterwick, L., and Smith, G. D. W. (1986). Aluminium Recovery from Consumer Waste-I. Technology Review. *Conservation & Recycling* 9, 281–292. doi:10.1016/0361-3658(86)90018-4
- Cai, Y., Kumar, S., Chua, R., Verma, V., Yuan, D., Kou, Z., et al. (2020). Bronze-type Vanadium Dioxide Holey Nanobelts as High Performing Cathode Material for Aqueous Aluminium-Ion Batteries. *J. Mater. Chem. A* 8, 12716–12722. doi:10.1039/D0TA03986A
- Chao, D., Zhou, W., Xie, F., Ye, C., Li, H., Jaroniec, M., et al. (2020). Roadmap for Advanced Aqueous Batteries: From Design of Materials to Applications. *Sci. Adv.* 6, 4098. doi:10.1126/sciadv.aba4098
- CHEMnetBASE (2016). *Abundance of Elements in the Earth's Crust and in the Sea*, 14–17. Available at: https://hbcpc.chemnetbase.com/faces/documents/14_10/14_10_0001.xhtml.
- Chen, J., Zhu, Q., Jiang, L., Liu, R., Yang, Y., Tang, M., et al. (2021). Rechargeable Aqueous Aluminum Organic Batteries. *Angew. Chem. Int. Ed.* 60, 605794–605799. doi:10.1002/anie.202011144
- Chen, L., Bao, J. L., Dong, X., Truhlar, D. G., Wang, Y., Wang, C., et al. (2017). Aqueous Mg-Ion Battery Based on Polyimide Anode and Prussian Blue Cathode. *ACS Energy Lett.* 2, 1115–1121. doi:10.1021/acsenerylett.7b00040
- Christensen, P. A., Anderson, P. A., Harper, G. D. J., Lambert, S. M., Mrozik, W., Rajaeifar, M. A., et al. (2021). Risk Management over the Life Cycle of Lithium-Ion Batteries in Electric Vehicles. *Renew. Sustain. Energy Rev.* 148, 111240. doi:10.1016/j.rser.2021.111240
- Ciez, R. E., and Whitacre, J. F. (2019). Examining Different Recycling Processes for Lithium-Ion Batteries. *Nat. Sustainability* 2, 148–156. doi:10.1038/s41893-019-0222-5
- Cresce, A., and Xu, K. (2021). Aqueous Lithium-ion Batteries. *Carbon Energy* 3, 721–751. doi:10.1002/cey2.106
- Das, S. K., Mahapatra, S., and Lahan, H. (2017). Aluminium-ion Batteries: Developments and Challenges. *J. Mater. Chem. A* 5, 6347–6367. doi:10.1039/C7TA00228A
- Dell, R. M. (1996). Aqueous Electrolyte Batteries. *Philos. Trans. Math. Phys. Eng. Sci.* 354, 1515–1527.
- Di Palma, T. M., Migliardini, F., Caputo, D., and Corbo, P. (2017). Xanthan and κ-carrageenan Based Alkaline Hydrogels as Electrolytes for Al/air Batteries. *Carbohydr. Polym.* 157, 122–127. doi:10.1016/j.carbpol.2016.09.076
- IPCCedenhofer, R., Pichs-Madruga, Y., Sokona, E., Farahani, S., Kadner, K., Seyboth, I. A. A., et al. (2014). *Climate Change 2014: Mitigation of Climate Change Contribution of Working Group III to the Fifth Assessment Report*. Cambridge, United Kingdom: Cambridge University Press.
- Elia, G. A., Kravchik, K. V., Kovalenko, M. V., Chacón, J., Holland, A., and Wills, R. G. A. (2021). An Overview and Prospective on Al and Al-Ion Battery Technologies. *J. Power Sourc.* 481, 228870. doi:10.1016/j.jpowsour.2020.228870
- Faegh, E., Ng, B., Hayman, D., and Mustain, W. E. (2021). Practical Assessment of the Performance of Aluminium Battery Technologies. *Nat. Energy* 6, 21–29. doi:10.1038/s41560-020-00728-y
- Gaele, M. F., Migliardini, F., and Di Palma, T. M. (2021). Dual Solid Electrolytes for Aluminium-Air Batteries Based on Polyvinyl Alcohol Acidic Membranes and Neutral Hydrogels. *J. Solid State. Electrochem.* 25, 1207–1216. doi:10.1007/s10008-021-04900-6
- Gao, Y., Yang, H., Wang, X., Bai, Y., Zhu, N., Guo, S., et al. (2020). The Compensation Effect Mechanism of Fe-Ni Mixed Prussian Blue Analogues in Aqueous Rechargeable Aluminum-Ion Batteries. *ChemSusChem* 13, 732–740. doi:10.1002/cssc.201903067
- Gheyfani, S., Liang, Y., Wu, F., Jing, Y., Dong, H., Rao, K. K., et al. (2017). An Aqueous Ca-Ion Battery. *Adv. Sci.* 4, 1700465. doi:10.1002/advs.201700465
- González, J. R., Nacimiento, F., Cabello, M., Alcántara, R., Lavela, P., and Tirado, J. L. (2016). Reversible Intercalation of Aluminium into Vanadium Pentoxide Xerogel for Aqueous Rechargeable Batteries. *RSC Adv.* 6, 62157–62164. doi:10.1039/C6RA11030D
- Gores, H. J., Barthel, J., Zugmann, S., Moosbauer, D., Amereller, M., Hartl, R., et al. (2011). “Liquid Nonaqueous Electrolytes,” in *Handbook of Battery Materials*. Editors C. Daniel and J. O. Besenhard (Hoboken, New Jersey, United States: John Wiley & Sons), 525, 626. doi:10.1002/9783527637188.ch17
- Gray, F., and Armand, M. (2011). “Polymer Electrolytes,” in *Handbook of Battery Materials*. Editors C. Daniel and J. O. Besenhard (Hoboken, New Jersey, United States: John Wiley & Sons), 627–656. doi:10.1002/9783527637188.ch18
- Gür, T. M. (2018). Review of Electrical Energy Storage Technologies, Materials and Systems: Challenges and Prospects for Large-Scale Grid Storage. *Energy Environ. Sci.* 11 (10), 2696–2767. doi:10.1039/C8EE01419A
- He, J., Shi, X., Wang, C., Zhang, H., Liu, X., Yang, Z., et al. (2021). A Quinone Electrode with Reversible Phase Conversion for Long-Life Rechargeable Aqueous Aluminum-Metal Batteries. *Chem. Commun.* 57, 576931–576934. doi:10.1039/D1CC02024B
- He, S., Wang, J., Zhang, X., Chen, J., Wang, Z., Yang, T., et al. (2019). A High-Energy Aqueous Aluminum-Manganese Battery. *Adv. Funct. Mater.* 29, 1905228. doi:10.1002/adfm.201905228
- Holland, A. (2018). “Development and Characterisation of an Aqueous Aluminium-Ion Battery,”. PhD Thesis (Southampton, England: University of Southampton).
- Holland, A., Kimpton, H., Cruden, A., and Wills, R. (2018c). CuHCF as an Electrode Material in an Aqueous Dual-Ion Al³⁺/K⁺ Ion Battery. *Energy Proced.* 151, 15169–15173. doi:10.1016/j.egypro.2018.09.029
- Holland, A., McKerracher, R. D., Cruden, A., and Wills, R. G. A. (2018b). An Aluminium Battery Operating with an Aqueous Electrolyte. *J. Appl. Electrochem.* 48, 48243–48250. doi:10.1007/s10800-018-1154-x
- Holland, A. W., Cruden, A., Zerey, A., Hector, A., and Wills, R. G. A. (2019). Electrochemical Study of TiO₂ in Aqueous AlCl₃ Electrolyte via Vacuum Impregnation for superior High-Rate Electrode Performance. *BMC Energy* 1, 10. doi:10.1186/s42500-019-0010-9
- Holland, A. W., McKerracher, R., Cruden, A., and Wills, R. G. A. (2018a). TiO₂ Nanopowder as a High Rate, Long Cycle Life Electrode in Aqueous Aluminium Electrolyte. *Mater. Today Energy* 10, 208–213. doi:10.1016/j.mtener.2018.09.009
- Hopkins, B. J., Shao-Horn, Y., and Hart, D. P. (2018). Suppressing Corrosion in Primary Aluminum-Air Batteries via Oil Displacement. *Science* 362, 362658–362661. doi:10.1126/science.aat9149
- Huang, B., Pan, Z., Su, X., and An, L. (2018). Recycling of Lithium-Ion Batteries: Recent Advances and Perspectives. *J. Power Sourc.* 399, 274–286. doi:10.1016/j.jpowsour.2018.07.116
- Javed, M. S., Lei, H., Wang, Z., Liu, B.-t., Cai, X., and Mai, W. (2020). 2D V₂O₅ Nanosheets as a Binder-free High-Energy Cathode for Ultrafast Aqueous and Flexible Zn-Ion Batteries. *Nano Energy* 70, 104573. doi:10.1016/j.nanoen.2020.104573
- Jiang, L., Lu, Y., Zhao, C., Liu, L., Zhang, J., Zhang, Q., et al. (2019). Building Aqueous K-Ion Batteries for Energy Storage. *Nat. Energy* 4, 495–503. doi:10.1038/s41560-019-0388-0
- Jin, B., Hejazi, S., Chu, H., Cha, G., Altomare, M., Yang, M., et al. (2021). A Long-Term Stable Aqueous Aluminum Battery Electrode Based on One-Dimensional Molybdenum-Tantalum Oxide Nanotube Arrays. *Nanoscale* 13, 6087–6095. doi:10.1039/D0NR08671A
- Jin, T., Ji, X., Wang, P. F., Zhu, K., Zhang, J., Cao, L., et al. (2021). High-Energy Aqueous Sodium-Ion Batteries. *Angew. Chem. Int. Ed.* 60, 6011943–6011948. doi:10.1002/anie.202017167
- Joseph, J., Fernando, J. F. S., Sayeed, M. A., Tang, C., Golberg, D., Du, A., et al. (2020). Exploring Aluminum-Ion Insertion into Magnesium-Doped Manjiroite (MnO₂) Nanorods in Aqueous Solution. *ChemElectroChem* 8, 1048–1054. doi:10.1002/celc.202001408
- Joseph, J., Nerkar, J., Tang, C., Du, A., O'Mullane, A. P., and Ostrikov, K. (2019a). Reversible Intercalation of Multivalent Al³⁺ Ions into Potassium-Rich Cryptomelane Nanowires for Aqueous Rechargeable Al-Ion Batteries. *ChemSusChem* 12, 3753–3760. doi:10.1002/cssc.201901182
- Joseph, J., O'Mullane, A. P., and Ostrikov, K. (2019b). Hexagonal Molybdenum Trioxide (h-MoO₃) as an Electrode Material for Rechargeable Aqueous Aluminum-Ion Batteries. *ChemElectroChem* 6, 6002–6008. doi:10.1002/celc.201901890

- Katsoufis, P., Katsaiti, M., Mourelas, C., Andrade, T. S., Dracopoulos, V., Politis, C., et al. (2020). Study of a Thin Film Aluminum-Air Battery. *Energies* 13, 1447. doi:10.3390/en13061447
- Kazazi, M., Abdollahi, P., and Mirzaei-Moghadam, M. (2017). High Surface Area TiO₂ Nanospheres as a High-Rate Anode Material for Aqueous Aluminium-Ion Batteries. *Solid State Ionics* 300, 32–37. doi:10.1016/j.ssi.2016.11.028
- Koketsu, T., Ma, J., Morgan, B. J., Body, M., Legein, C., Dachraoui, W., et al. (2017). Reversible Magnesium and Aluminium Ions Insertion in Cation-Deficient Anatase TiO₂. *Nat. Mater* 16, 161142–161148. doi:10.1038/nmat4976
- Kong, B., Tang, J., Wu, Z., Wei, J., Wu, H., Wang, Y., et al. (2014). Ultralight Mesoporous Magnetic Frameworks by Interfacial Assembly of Prussian Blue Nanocubes. *Angew. Chem. Int. Ed.* 53, 2888–2892. doi:10.1002/anie.201308625
- Krishnamoorthy, M., and Jha, N. (2019). Oxygen-Rich Hierarchical Porous Graphene as an Excellent Electrode for Supercapacitors, Aqueous Al-Ion Battery, and Capacitive Deionization. *ACS Sustain. Chem. Eng.* 7, 8475–8489. doi:10.1021/acssuschemeng.9b00233
- Kumar, S., Satish, R., Verma, V., Ren, H., Kidkhunthod, P., Manalastas, W., et al. (2019). Investigating FeVO₄ as a Cathode Material for Aqueous Aluminium-Ion Battery. *J. Power Sourc.* 426, 426151–426161. doi:10.1016/j.jpowsour.2019.03.119
- Lahan, H., Boruah, R., Hazarika, A., and Das, S. K. (2017). Anatase TiO₂ as an Anode Material for Rechargeable Aqueous Aluminium-Ion Batteries: Remarkable Graphene Induced Aluminium Ion Storage Phenomenon. *J. Phys. Chem. C* 121, 12126241–12126249. doi:10.1021/acs.jpcc.7b09494
- Lahan, H., and Das, S. K. (2019a). Al³⁺ Ion Intercalation in MoO₃ for Aqueous Aluminium-Ion Battery. *J. Power Sourc.* 413, 413134–413138. doi:10.1016/j.jpowsour.2018.12.032
- Lahan, H., and Das, S. K. (2018). An Approach to Improve the Al³⁺ Ion Intercalation in Anatase TiO₂ Nanoparticle for Aqueous Aluminium-Ion Battery. *Ionics* 24, 1855–1860. doi:10.1007/s11581-018-2530-6
- Lahan, H., and Das, S. K. (2019b). Reversible Al³⁺ Ion Insertion into Tungsten Trioxide (WO₃) for Aqueous Aluminium-Ion Batteries. *Dalton Trans.* 48, 6337–6340. doi:10.1039/C9DT00844F
- Larcher, D., and Tarascon, J. M. (2015). Towards Greener and More Sustainable Batteries for Electrical Energy Storage. *Nat. Chem.* 7, 19–29. doi:10.1038/nchem.2085
- Larsson, F., Bertilsson, S., Furlani, M., Albinsson, I., and Mellander, B.-E. (2018). Gas Explosions and Thermal Runaways during External Heating Abuse of Commercial Lithium-Ion Graphite-LiCoO₂ Cells at Different Levels of Ageing. *J. Power Sourc.* 373, 220–231. doi:10.1016/j.jpowsour.2017.10.085
- Li, J., Chen, J., Wan, H., Xiao, J., Tang, Y., Liu, M., et al. (2019). Boosting Oxygen Reduction Activity of Fe-N-C by Partial Copper Substitution to Iron in Al-Air Batteries. *Appl. Catal. B: Environ.* 242, 209–217. doi:10.1016/j.apcatb.2018.09.044
- Li, Y., Liu, L., Lu, Y., Shi, R., Ma, Y., Yan, Z., et al. (2021). High-Energy-Density Quinone-Based Electrodes with [Al(OTF)]²⁺ Storage Mechanism for Rechargeable Aqueous Aluminum Batteries. *Adv. Funct. Mater.* 31, 2102063. doi:10.1002/adfm.202102063
- Li, Z., Xiang, K., Xing, W., Carter, W. C., and Chiang, Y.-M. (2015). Reversible Aluminium-Ion Intercalation in Prussian Blue Analogs and Demonstration of a High-Power Aluminum-Ion Asymmetric Capacitor. *Adv. Energ. Mater.* 5, 1401410. doi:10.1002/aenm.201401410
- Liu, S., Hu, J. J., Yan, N. F., Pan, G. L., Li, G. R., and Gao, X. P. (2012). Aluminum Storage Behavior of Anatase TiO₂ Nanotube Arrays in Aqueous Solution for Aluminum Ion Batteries. *Energ. Environ. Sci.* 5, 9743–9746. doi:10.1039/c2ee22987k
- Liu, S., Pan, G. L., Li, G. R., and Gao, X. P. (2015). Copper Hexacyanoferrate Nanoparticles as Cathode Material for Aqueous Al-Ion Batteries. *J. Mater. Chem. A* 3, 959–962. doi:10.1039/C4TA04644G
- Liu, S., Ye, S. H., Li, C. Z., Pan, G. L., and Gao, X. P. (2011). Rechargeable Aqueous Lithium-Ion Battery of TiO₂/LiMn₂O₄ with a High Voltage. *J. Electrochem. Soc.* 158, A1490–A1497. doi:10.1149/2.094112jes
- Liu, X., Zhang, P., and Xue, J. (2019). The Role of Micro-naoscale AlSb Precipitates in Improving the Discharge Performance of Al-Sb alloy Anodes for Al-Air Batteries. *J. Power Sourc.* 425, 186–194. doi:10.1016/j.jpowsour.2019.04.012
- Liu, X., Zhang, P., Xue, J., Zhu, C., Li, X., and Wang, Z. (2021). High Energy Efficiency of Al-Based Anodes for Al-Air Battery by Simultaneous Addition of Mn and Sb. *Chem. Eng. J.* 417, 128006. doi:10.1016/j.cej.2020.128006
- Liu, Y., Sang, S., Wu, Q., Lu, Z., Liu, K., and Liu, H. (2014). The Electrochemical Behavior of Cl⁻ Assisted Al³⁺ Insertion into Titanium Dioxide Nanotube Arrays in Aqueous Solution for Aluminum Ion Batteries. *Electrochimica Acta* 143, 340–346. doi:10.1016/j.electacta.2014.08.016
- Liu, Y., Yang, L., Xie, B., Zhao, N., Yang, L., Zhan, F., et al. (2020). Ultrathin Co₃O₄ Nanosheet Clusters Anchored on Nitrogen Doped Carbon nanotubes/3D Graphene as Binder-free Cathodes for Al-Air Battery. *Chem. Eng. J.* 381, 122681. doi:10.1016/j.cej.2019.122681
- Maxwell, P. (2015). Transparent and Opaque Pricing: The Interesting Case of Lithium. *Resour. Pol.* 45, 92–97. doi:10.1016/j.resourpol.2015.03.007
- Mohanapriya, K., and Jha, N. (2019). Hierarchically Hybrid Nanostructure of Carbon Nanoparticles Decorated Graphene Sheets as an Efficient Electrode Material for Supercapacitors, Aqueous Al-Ion Battery and Capacitive Deionization. *Electrochimica Acta* 324, 134870. doi:10.1016/j.electacta.2019.134870
- Mutlu, R. N., Ateş, S., and Yazıcı, B. (2017). Al-6013-T6 and Al-7075-T7351 alloy Anodes for Aluminium-Air Battery. *Int. J. Hydrogen Energy* 42, 23315–23325. doi:10.1016/j.ijhydene.2017.02.136
- Mutlu, R. N., and Yazıcı, B. (2019). Copper-deposited Aluminum Anode for Aluminum-Air Battery. *J. Solid State. Electrochem.* 23, 529–541. doi:10.1007/s10008-018-4146-1
- Nacimiento, F., Cabello, M., Alcántara, R., Lavela, P., and Tirado, J. L. (2018). NASICON-type Na₃V₂(PO₄)₃ as a New Positive Electrode Material for Rechargeable Aluminium Battery. *Electrochimica Acta* 260, 260798–260804. doi:10.1016/j.electacta.2017.12.040
- Nandi, S., and Das, S. K. (2020). An Electrochemical Study on Bismuth Oxide (Bi₂O₃) as an Electrode Material for Rechargeable Aqueous Aluminium-Ion Battery. *Solid State Ionics* 347, 115228. doi:10.1016/j.ssi.2020.115228
- Nandi, S., Lahan, H., and Das, S. K. (2019). A Proof of Concept for Low-Cost Rechargeable Aqueous Aluminium-Ion Batteries. *Bull. Mater. Sci.* 43, 43–26. doi:10.1007/s12034-019-1988-9
- Narins, T. P. (2017). The Battery Business: Lithium Availability and the Growth of the Global Electric Car Industry. *Extractive Industries Soc.* 4, 321–328. doi:10.1016/j.exis.2017.01.013
- Palanisamy, S., Rajendhran, N., Srinivasan, S., Shyma, A. P., Murugan, V., Parasuraman, B., et al. (2020). A Novel Nano-YSZ-Al alloy Anode for Al-Air Battery. *J. Appl. Electrochem.* 51, 345–356. doi:10.1007/s10800-020-01493-2
- Pang, Q., Yang, S., Yu, X., He, W., Zhang, S., Tian, Y., et al. (2021). Realizing Reversible Storage of Trivalent Aluminum Ions Using VOPO₄·2H₂O Nanosheets as Cathode Material in Aqueous Aluminum Metal Batteries. *J. Alloys Compd.* 885, 161008. doi:10.1016/j.jallcom.2021.161008
- Parvizi, P., and Kazazi, M. (2018). Binder-free Copper Hexacyanoferrate Electrode Prepared by Pulse Galvanostatic Electrochemical Deposition for Aqueous-Based Al-Ion Batteries. *Adv. Ceramics Prog.* 4, 27–31. doi:10.30501/acp.2018.91122
- Pino, M., Herranz, D., Chacón, J., Fatás, E., and Ocón, P. (2016). Carbon Treated Commercial Aluminium Alloys as Anodes for Aluminium-Air Batteries in Sodium Chloride Electrolyte. *J. Power Sourc.* 326, 326296–326302. doi:10.1016/j.jpowsour.2016.06.118
- Posada, J. O. G., Rennie, A. J. R., Villar, S. P., Martins, V. L., Marinaccio, J., Barnes, A., et al. (2017). Aqueous Batteries as Grid Scale Energy Storage Solutions. *Renew. Sustain. Energ. Rev.* 68, 1174–1182. doi:10.1016/j.rser.2016.02.024
- Prior, T., Wäger, P. A., Stamp, A., Widmer, R., and Giurco, D. (2013). Sustainable Governance of Scarce Metals: The Case of Lithium. *Sci. Total Environ.* 461–462, 461785–462791. doi:10.1016/j.scitotenv.2013.05.042
- Ru, Y., Zheng, S., Xue, H., and Pang, H. (2020). Potassium Cobalt Hexacyanoferrate Nanocubic Assemblies for High-Performance Aqueous Aluminium Ion Batteries. *Chem. Eng. J.* 382, 122853. doi:10.1016/j.cej.2019.122853
- Ryu, J., Jang, H., Park, J., Yoo, Y., Park, M., and Cho, J. (2018). Seed-mediated Atomic-Scale Reconstruction of Silver Manganate Nanoplates for Oxygen Reduction towards High-Energy Aluminium-Air Flow Batteries. *Nat. Commun.* 9, 3715. doi:10.1038/s41467-018-06211-3
- Smith, B. D., Wills, R. G. A., and Cruden, A. J. (2020). Aqueous Al-Ion Cells and Supercapacitors - A Comparison. *Energ. Rep.* 6, 166–173. doi:10.1016/j.egy.2020.03.021
- Song, M., Tan, H., Chao, D., and Fan, H. J. (2018). Recent Advances in Zn-Ion Batteries. *Adv. Funct. Mater.* 28, 1802564. doi:10.1002/adfm.201802564
- Suo, L., Borodin, O., Gao, T., Olguin, M., Ho, J., Fan, X., et al. (2015). "Water-in-salt" Electrolyte Enables High-Voltage Aqueous Lithium-Ion Chemistries. *Science* 350, 350938–350943. doi:10.1126/science.aab1595
- Suo, L., Borodin, O., Wang, Y., Rong, X., Sun, W., Fan, X., et al. (2017). "Water-in-Salt" Electrolyte Makes Aqueous Sodium-Ion Battery Safe, Green, and Long-Lasting. *Adv. Energ. Mater.* 7, 1701189. doi:10.1002/aenm.201701189

- Takeda, Y., and Taguchi, K. (2018). Proposal of NaAlO₂ as an Electrolyte of Aluminum-Air Battery. *J. Fundam. Appl. Sci.* 10.
- Tang, W., Xuan, J., Wang, H., Zhao, S., and Liu, H. (2018). First-principles Investigation of Aluminum Intercalation and Diffusion in TiO₂ Materials: Anatase versus Rutile. *J. Power Sourc.* 384, 384249–384255. doi:10.1016/j.jpowsour.2018.02.088
- Tang, W., Zhu, Y., Hou, Y., Liu, L., Wu, Y., Loh, K. P., et al. (2013). Aqueous Rechargeable Lithium Batteries as an Energy Storage System of Superfast Charging. *Energy Environ. Sci.* 6, 2093–2104. doi:10.1039/c3ee24249h
- Tapia-Ruiz, N., Armstrong, A. R., Alptekin, H., Amores, M. A., Au, H., Barker, J., et al. (2021/2021). 2021 Roadmap for Sodium-Ion Batteries. *J. Phys. Energy* 3, 031503. doi:10.1088/2515-7655/ac01ef
- Teabnamang, P., Kao-ian, W., Nguyen, M. T., Yonezawa, T., Cheacharoen, R., and Kheawhom, S. (2020). High-Capacity Dual-Electrolyte Aluminum-Air Battery with Circulating Methanol Anolyte. *Energies* 13, 2275. doi:10.3390/en13092275
- Thalji, M. R., Ali, G. A. M., Liu, P., Zhong, Y. L., and Chong, K. F. (2021). W18O₄₉ Nanowires-Graphene Nanocomposite for Asymmetric Supercapacitors Employing AlCl₃ Aqueous Electrolyte. *Chem. Eng. J.* 409, 128216. doi:10.1016/j.cej.2020.128216
- Tian, M., Li, R., Liu, C., Long, D., and Cao, G. (2019). Aqueous Al-Ion Supercapacitor with V₂O₅ Mesoporous Carbon Electrodes. *ACS Appl. Mater. Inter.* 11, 15573–15580. doi:10.1021/acsami.9b02030
- UK Government (2008). *Climate Change Act 2008*. Available at: <https://www.legislation.gov.uk/ukpga/2008/27/contents>.
- UK Government (2019). *UK Energy Statistics, Q1*. Available at: https://assets.publishing.service.gov.uk/government/uploads/system/uploads/attachment_data/file/812626/Press_Notice_June_19.pdf.
- United States Department of Energy (2019). *Energy Storage Technology and Cost Characterization Report*. Available at: <https://energystorage.pnnl.gov/pdf/PNNL-28866.pdf>.
- USGS (2020). *Mineral Commodity Summaries, 200*. Available at: <https://pubs.usgs.gov/periodicals/mcs2020/mcs2020.pdf>.
- Wang, L., Fu, L., Li, J., Zeng, X., Xie, H., Huang, X., et al. (2018). On an Easy Way to Prepare Highly Efficient Fe/N-Co-Doped Carbon Nanotube/nanoparticle Composite for Oxygen Reduction Reaction in Al-Air Batteries. *J. Mater. Sci.* 53, 10280–10291. doi:10.1007/s10853-018-2245-0
- Wang, P., Chen, Z., Ji, Z., Feng, Y., Wang, J., Liu, J., et al. (2019). A Flexible Aqueous Al Ion Rechargeable Full Battery. *Chem. Eng. J.* 373, 580–586. doi:10.1016/j.cej.2019.05.085
- Wang, P., Chen, Z., Wang, H., Ji, Z., Feng, Y., Wang, J., et al. (2020). A High-Performance Flexible Aqueous Al Ion Rechargeable Battery with Long Cycle Life. *Energy Storage Mater.* 25, 426–435. doi:10.1016/j.ensm.2019.09.038
- Wang, Q., Miao, H., Xue, Y., Sun, S., Li, S., and Liu, Z. (2017). Performances of an Al-0.15 Bi-0.15 Pb-0.035 Ga alloy as an Anode for Al-Air Batteries in Neutral and Alkaline Electrolytes. *RSC Adv.* 7, 25838–25847. doi:10.1039/C7RA02918G
- Wessells, C. D., Peddada, S. V., McDowell, M. T., Huggins, R. A., and Cui, Y. (2011). The Effect of Insertion Species on Nanostructured Open Framework Hexacyanoferrate Battery Electrodes. *J. Electrochem. Soc.* 159, A98–A103. doi:10.1149/2.060202jes
- Wu, B., Wu, Y., Lu, Z., Zhang, J., Han, N., Wang, Y., et al. (2021). A Cation Selective Separator Induced Cathode Protective Layer and Regulated Zinc Deposition for Zinc Ion Batteries. *J. Mater. Chem. A* 9, 4734–4743. doi:10.1039/D0TA11841A
- Wu, C., Gu, S., Zhang, Q., Bai, Y., Li, M., Yuan, Y., et al. (2019). Electrochemically Activated Spinel Manganese Oxide for Rechargeable Aqueous Aluminum Battery. *Nat. Commun.* 10, 73. doi:10.1038/s41467-018-07980-7
- Wu, S., Zhang, Q., Sun, D., Luan, J., Shi, H., Hu, S., et al. (2020). Understanding the Synergistic Effect of Alkyl Polyglucoside and Potassium Stannate as Advanced Hybrid Corrosion Inhibitor for Alkaline Aluminum-Air Battery. *Chem. Eng. J.* 383, 123162. doi:10.1016/j.cej.2019.123162
- Wu, X., Qin, N., Wang, F., Li, Z., Qin, J., Huang, G., et al. (2021). Reversible Aluminum Ion Storage Mechanism in Ti-Deficient Rutile Titanium Dioxide Anode for Aqueous Aluminum-Ion Batteries. *Energy Storage Mater.* 37, 619–627. doi:10.1016/j.ensm.2021.02.040
- Wu, Z., Zhang, H., Guo, C., Zou, J., Qin, K., Ban, C., et al. (2019). Effects of Indium, Gallium, or Bismuth Additions on the Discharge Behavior of Al-Mg-Sn-Based alloy for Al-Air Battery Anodes in NaOH Electrolytes. *J. Solid State Electrochem.* 23, 2483–2491. doi:10.1007/s10008-019-04341-2
- Xia, M., Zhang, X., Liu, T., Yu, H., Chen, S., Peng, N., et al. (2020). Commercially Available Prussian Blue Get Energetic in Aqueous K-Ion Batteries. *Chem. Eng. J.* 394, 124923. doi:10.1016/j.cej.2020.124923
- Xue, Y., Miao, H., Sun, S., Wang, Q., Li, S., and Liu, Z. (2017). La_{1-x}Ag_xMnO₃ Electrocatalyst with High Catalytic Activity for Oxygen Reduction Reaction in Aluminum Air Batteries. *RSC Adv.* 7, 5214–5221. doi:10.1039/C6RA25242G
- Yan, C., Lv, C., Wang, L., Cui, W., Zhang, L., Dinh, K. N., et al. (2020). Architecting a Stable High-Energy Aqueous Al-Ion Battery. *J. Am. Chem. Soc.* 142, 14215295–14215304. doi:10.1021/jacs.0c05054
- Yan, L., Zeng, X., Zhao, S., Jiang, W., Li, Z., Gao, X., et al. (2021). 9,10-Anthraquinone/K₂CuFe(CN)₆: A Highly Compatible Aqueous Aluminum-Ion Full-Battery Configuration. *ACS Appl. Mater. Inter.* 13, 8353–8360. doi:10.1021/acsami.0c20543
- Yang, C., Chen, J., Qing, T., Fan, X., Sun, W., von Cresce, A., et al. (2017). 4.0 V Aqueous Li-Ion Batteries. *Joule* 1, 122–132. doi:10.1016/j.joule.2017.08.009
- Yu, Y., Chen, M., Wang, S., Hill, C., Joshi, P., Kuruganti, T., et al. (2018). Laser Sintering of Printed Anodes for Al-Air Batteries. *J. Electrochem. Soc.* 165, A584–A592. doi:10.1149/2.0811803jes
- Zhang, H., Liu, X., Li, H., Hasa, I., and Passerini, S. (2020). Challenges and Strategies for High-Energy Aqueous Electrolyte Rechargeable Batteries. *Angew. Chem. Int. Ed.* 60, 598–616. doi:10.1002/anie.202004433
- Zhang, P., Liu, X., Xue, J., and Jiang, K. (2020). The Role of Microstructural Evolution in Improving Energy Conversion of Al-Based Anodes for Metal-Air Batteries. *J. Power Sourc.* 451, 227806. doi:10.1016/j.jpowsour.2020.227806
- Zhang, P., Liu, X., Xue, J., and Wang, Z. (2019). Evaluating the Discharge Performance of Heat-Treated Al-Sb Alloys for Al-Air Batteries. *J. Mater. Eng. Perform.* 28, 5476–5484. doi:10.1007/s11665-019-04287-6
- Zhao, Q., Liu, L., Yin, J., Zheng, J., Zhang, D., Chen, J., et al. (2020). Proton Intercalation/De-Intercalation Dynamics in Vanadium Oxides for Aqueous Aluminum Electrochemical Cells. *Angew. Chem. Int. Ed.* 59, 3048–3052. doi:10.1002/anie.201912634
- Zhao, Q., Zachman, M. J., Al Sadat, W. I., Zheng, J., Kourkoutis, L. F., and Archer, L. (2018). Solid Electrolyte Interphases for High-Energy Aqueous Aluminum Electrochemical Cells. *Sci. Adv.* 4, eaau8131. doi:10.1126/sciadv.aau8131
- Zhao, T., Ojeda, M., Xuan, J., Shu, Z., and Wang, H. (2019). Aluminum Storage in Rutile-Based TiO₂ Nanoparticles. *Energy Proced.* 158, 4829–4833. doi:10.1016/j.egypro.2019.01.712
- Zhong, W., Sang, S., Liu, Y., Wu, Q., Liu, K., and Liu, H. (2015). Electrochemically Conductive Treatment of TiO₂ Nanotube Arrays in AlCl₃ Aqueous Solution for Supercapacitors. *J. Power Sourc.* 294, 216–222. doi:10.1016/j.jpowsour.2015.06.052
- Zhou, A., Jiang, L., Yue, J., Tong, Y., Zhang, Q., Lin, Z., et al. (2019). Water-in-Salt Electrolyte Promotes High-Capacity FeFe(CN)₆ Cathode for Aqueous Al-Ion Battery. *ACS Appl. Mater. Inter.* 11, 41356–41362. doi:10.1021/acsami.9b14149
- Znaidi, L., Baffier, N., and Huber, M. (1989). Synthesis of Vanadium Bronzes MxV₂O₅ through Sol-Gel Processes I - Monoclinic Bronzes (M = Na, Ag). *Mater. Res. Bull.* 24, 1501–1514. doi:10.1016/0025-5408(89)90161-X

Conflict of Interest: The authors declare that the research was conducted in the absence of any commercial or financial relationships that could be construed as a potential conflict of interest.

Publisher's Note: All claims expressed in this article are solely those of the authors and do not necessarily represent those of their affiliated organizations or those of the publisher, the editors, and the reviewers. Any product that may be evaluated in this article, or claim that may be made by its manufacturer, is not guaranteed or endorsed by the publisher.

Copyright © 2022 Melzack and Wills. This is an open-access article distributed under the terms of the Creative Commons Attribution License (CC BY). The use, distribution or reproduction in other forums is permitted, provided the original author(s) and the copyright owner(s) are credited and that the original publication in this journal is cited, in accordance with accepted academic practice. No use, distribution or reproduction is permitted which does not comply with these terms.